SEE/CR-2004-400

Meteoroid Engineering Model – Final Report

J. Jones
University of Western Ontario, London, Ontario

National Aeronautics and
Space Administration

Marshall Space Flight Center • MSFC, Alabama 35812

June 2004

Meteoroid Engineering Model – Final Report

J. Jones Department of Physics and Astronomy
University of Western Ontario
London, Ontario, Canada. N6A 3K7

Last revision: June 28, 2004

Summary

We developed a parametric model of the spatial distribution of sporadic meteoroids by taking their primary source to be short-period comets with aphelia less than 7 AU which showed to be the major source of dust released through the sublimation of cometary ices. We constrained the model to fit the observed distribution of particles deduced from the zodiacal light measurements of Helios I and II as well as Earth-based radio-meteor observations. We also considered the contribution to the sporadic meteor complex from long-period comets. An origin for the North and South Toroidal source of sporadic meteors is proposed and the results of calculations for the likely characteristics of asteroidal meteors are also presented. Predicted fluxes and radiant distributions of sporadic meteors in the region between Mercury and Mars are shown as well. We have also included the effects of the gravitational shielding and focussing of the planets and shown that flux enhancements of up to 70% are possible at some locations.

1. Background

Meteoroid impacts pose a significant hazard to spacecraft and while there is a considerable body of knowledge concerning the extent of this hazard close to the Earth, the situation elsewhere in the solar system is much less well-defined. This report describes an attempt to extend our knowledge of the meteoroid population within the inner solar system. Clearly some regions are presently inaccessible and since we have no information of the meteoroid environment there, perhaps the most we can hope for is a model that encompasses the region bounded by Mercury and Mars.

Meteoroids can be conveniently divided into two classes: stream and sporadic. Stream meteoroids move in highly collimated orbits that result in greatly enhanced localized particle fluxes that may be also time-dependent. When the Earth passes through such a

stream, a meteor shower or even a storm is observed. Sporadic meteors on the other hand can be thought of as a diffuse background of meteoroid activity. In this report we will be concerned with modeling the sporadic meteoroid complex. The reason for this is simple - sporadic meteoroids constitute the greater impact hazard to space vehicles. Although the mean sporadic meteoroid activity is low compared with that of stream meteoroids at the peak of a shower, it is present continuously throughout the year and as a result the integrated number of sporadic meteoroids far outweighs that of shower meteoroids. The mean rate of sporadic meteors is probably an order of magnitude greater than that of shower meteors.

The “Interplanetary Dust Model” of Grün, Zook, Fechtig and Giese (1985) has the advantage of simplicity and fits accurately the measured dust fluxes in the vicinity of the Earth's orbit but contains no directional information. Perhaps the most ambitious attempt to construct a model of the interplanetary dust complex is that of Devine (1993) who obtained empirical fits for the orbital distributions of the particles using observations from a wide variety of sources including zodiacal light, impact data and observations of radio-meteors. Devine's aim was to describe as accurately as possible the orbital distribution of interplanetary particles but because of the diverse nature of the data sources and the incompleteness of the measurements, a full solution was impossible without simplifying assumptions. For example, the most precise orbital data was provided by the Harvard Radio Meteor Project which, by its very nature, was restricted to particles whose orbits intersected the Earth's, leaving much of the inner solar system unsampled so that Devine had to rely on interpolation methods for the unsampled regions. Recently Taylor (1995) discovered an error due to a typographic mistake in the de-biasing of the speed distributions that raises questions about the reliability of Devine's model since his “core” distribution relied heavily on the radio-meteor data. Devine's model involved complicated analytic mathematics and because in its original form it was difficult to use, Garret, Drouilhet, Oliver and Evans (1999) and even more recently Jehn (2000) have simplified it.

There is clearly a need for a simple and easy-to-use model of the sporadic meteoroid complex. Rather than follow Devine, we have taken the path opened by Leinert *et al* (1983) and tried to develop a physically based model. Of course our knowledge of the system is far from complete but our philosophy has been to use the measurements to constrain the physical model rather than to build the model based on observations alone. In essence, we have tried to use our knowledge of the physical processes as the basis for our interpolations. We have tried to construct a model that is able to predict the concentration and velocity distribution of meteoroids within the greater part of the inner solar system. Our task has been to determine the orbital distribution of the meteoroids within this region.

Although the detailed calculation of the orbits of meteor stream particles is an extremely time-consuming task, for sporadic meteoroids we can start by making a number of simplifying assumptions - e.g. we can assume azimuthal symmetry about the ecliptic pole, and later, as the need arises, we can refine our model. If our model is to be considered reliable it must predict distributions of radiants and velocities similar to those

of sporadic meteors observed from the Earth. This paper describes our model of the sporadic meteoroid complex model and corresponds most closely with what Devine called his 'core' component, in as much as our model, being based on radio-meteor observations, refers to the mass range 10^{-5} - 1 g.

In the subsequent sections of this paper we first discuss general considerations for the distributions of interplanetary dust in the size range that can be accessed by meteor radars and which constitutes a significant hazard to space vehicles. We consider comets to be the primary source of this dust and show that the short-period comets are the predominant source. We first show how we have constructed a model of the equilibrium dust distribution due to short-period comets and how we have dealt with the uncertainty of the orbital distribution of the source and have included the results of the zodiacal light studies of Helios I and Helios II. We have included catastrophic collisions as well as the Poynting-Robertson effect in a parametric model which we have fitted to very recent observations made with the CMOR radar that have been corrected for the initial radius effect. We have also considered the dust produced by long-period comets, which present other problems. Here too we able to get good agreement with observations. The Northern and Southern Toroidal sources are very poorly defined but we have presented a tentative orbital distribution consistent with the radar observations. We have also examined the case of asteroidal meteors using as our starting point infra red observations provide by J.C. Liou. We find that asteroidal meteors are likely to be extremely difficult to observe using Earth-based meteor radar. Finally we treat the case of gravitational shielding and focussing by planets and have incorporated it into our model.

2. Determination of the particle concentration from the orbital distribution

Observations of the zodiacal light, (Leinert *et al*, 1983) indicate that the orbital distribution of interplanetary particles has azimuthal symmetry and can therefore be considered separable into a part, N(Q,q) that depends only on Q and q, the aphelion, and perihelion distances and a part that depends only on the orbital inclination. Initially we are concerned only with N(Q,q) since this determines the concentration of meteoroids, S(r), as a function of distance, r, from the Sun, through the standard expression given by Opik (1951), Kessler, (1981) and Steel and Elford (1986):

$$S(r) \propto \frac{1}{r} \iint \frac{N(Q,q)}{(Q+q)\sqrt{(r-q)(Q-r)}}\, dQ\, dq \qquad (2.1)$$

The zodiacal light observations by a number of space probes, notably Helios I and II, show strong evidence that the density of interplanetary dust varies with distance from the Sun as $r^{-1.3}$ (Leinert *et al*, 1981). Although the size of the particles responsible for the zodiacal light are somewhat smaller than typical meteoroids (10^{-4} m as compared with 10^{-3} m) they are not so small as to be removed by radiation pressure and are expected to show the same variation with distance from the Sun as meteoroids (Grün *et al*, 1985). It is

clear that the $r^{-1.3}$ dependence is insufficient to determine N(Q,q) uniquely and Leinert *et al* (1983) have presented several plausible distributions.

In the next section we examine the suggested sources and try to supply the additional information needed to specify N(Q,q).

3. Relative importance of cometary sources

To estimate the meteoroid space hazard from sporadic meteoroids we need to know relative importance of the various sources of meteoric material. It is generally accepted that meteoroids are either the result of the disintegration of comets or the products of asteroidal collisions. Comets either belong to the long or short-period groups depending on whether their orbital periods are longer or shorter than 200 years. But the period is not the only discriminant between these two groups - the short-period orbits are closely aligned with the ecliptic while the long-period orbits are essentially isotropical distributed. Within the short-period group there are two main families: the Jupiter family of comets with periods less than 20 yr and Tisserand parameters greater than 2.0 and the Halley family with periods greater than 20 yr and Tisserand parameters less than 2.0. In this section we estimate the production rate of meteoric material from each of these groups of comets and postpone for the moment the discussion of the asteroidal production of meteoric material.

Comets are not all the same size but we will assume that their orbital distributions are independent of mass and indeed Hughes (1987) has shown that for the most part the mass distributions of long and short-period comets are very similar. We can therefore ignore size-dependent effects. We will also assume that the composition of the comets is uniform so that the ratio of dust to ice is substantially constant. This allows us to take the amount of meteoric material released to be proportional to the amount of ice sublimated as the comet passes close to the Sun.

A comet far from the Sun re-radiates most of the energy it receives from the Sun while when it is close to the Sun most of the incident solar radiation on the unshielded areas goes into the sublimation of the cometary ices. Calculations by many authors (Delsemme, 1977; Jones, 1995) have shown that the dividing line is close to 2.3 AU. When the comet is closer to the Sun than 2.3 AU, sublimation predominates otherwise radiation is the major mechanism of heat loss and sublimation of water ice can usually be neglected. The true anomaly, θ_c, at which the distance to the Sun is 2.3 AU is given by

$$\cos(\theta_c) = \frac{0.435\ q\ (1+e) - 1}{e} \qquad (3.1)$$

where q is the perihelion distance and e the orbital eccentricity.
It is easily shown that the amount of ice sublimated per orbit and therefore the amount of meteoric material, P_{orbit} is

$$P_{orbit} \propto \frac{\theta_c}{\sqrt{q(1+e)}} \tag{3.2}$$

Similarly the average rate of production P_{avg}, is

$$P_{avg} \propto \frac{\theta_c (1-e)^2}{q^2 \sqrt{1-e^2}} \tag{3.3}$$

Applying these formulae to the comets from Marsden's catalogue that survived after we had removed duplicates corresponding to multiple apparitions, we obtained the results presented in Figure 3.1.

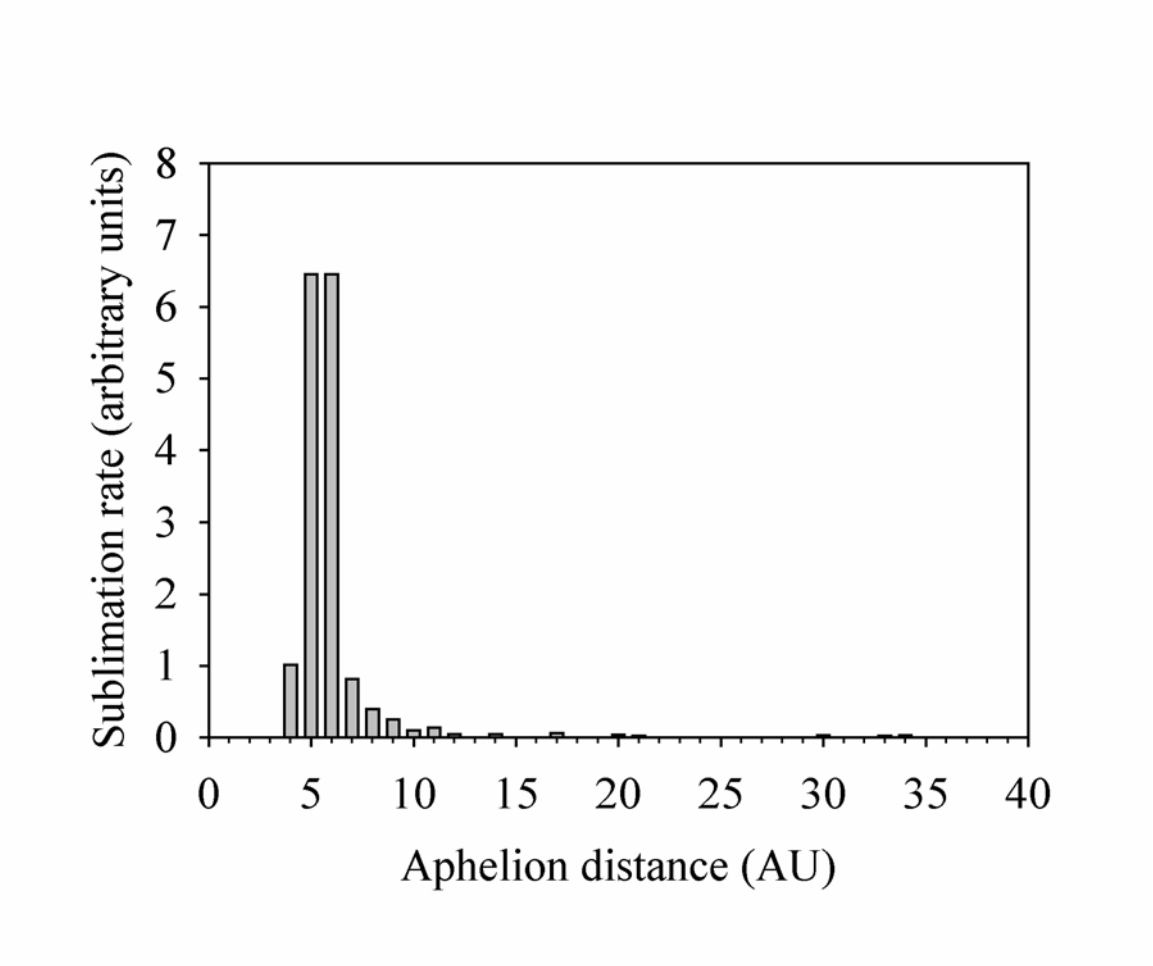

Figure 3.1 Sublimation rate versus aphelion distance for short-period comets

Table 3.1 Meteoroid production rates

Comet group	Percentage of total
Jupiter family	91
Halley family	5
Long-period	4

The majority of the integrated sublimation (see Table 3.1) is from short-period comets with aphelia less than 7AU which constitute a subset of the Jupiter family. We will designate these as the JF_m group, the subscript signifying that it is these comets which are presently the major source of meteoroids. The remaining sublimation is about equal to that from long-period comets. In Figure 3.2 we show the peri/aphelion distribution for those comets in the JF_m group.

We note that because of the relatively short period over which systematic observations have been made (about 200 years) and the small number of long-period comets (44) we estimated the contribution from this class of comets on the assumption that on average there is one apparition of a long-period comet every five years. It is clear that if comets are the major source of meteoric material, the overwhelming proportion of this will be produced by comets from the JF_m group.

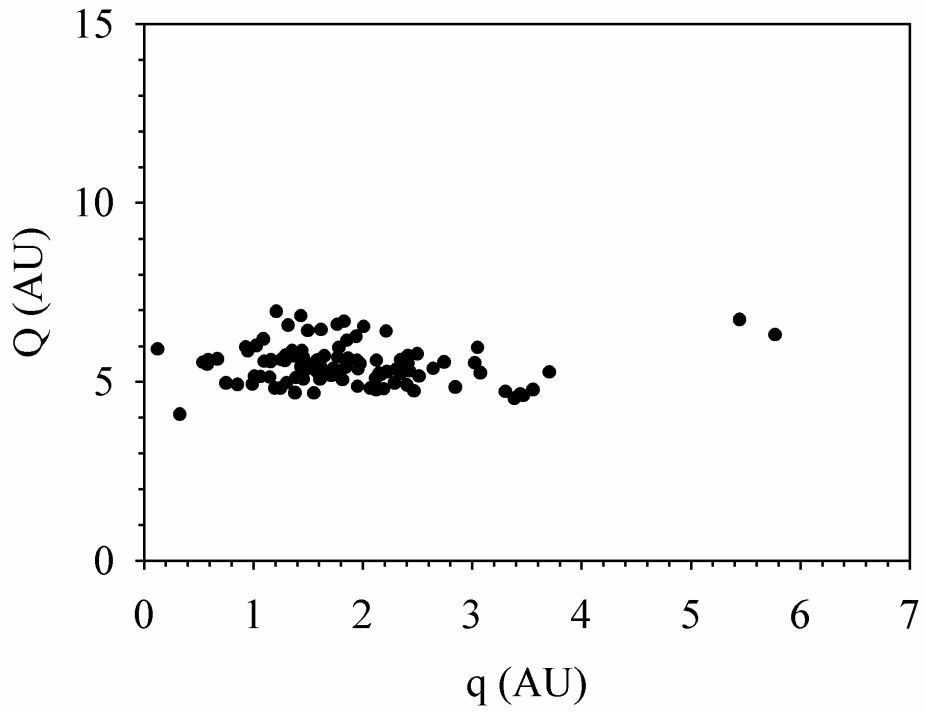

Figure 3.2 Peri/aphelion distributions of JF_m comets

4. Orbital parameters of the JF_m comets

Figure 2 shows a plot of aphelion versus perihelion distance for the JF_m comets and it is clear that the aphelia of these comets are clustered around the orbit of Jupiter itself and the mean values for the various orbital elements are given in Table 1.

We note that whereas the Jupiter family of short-period comets is usually defined in terms of the Tisserand parameter such that $2 < T < 3$, the meteoroid-producing comets are a subgroup of this family with T close to 2.80. On the other hand the perihelion distances appear to encompass a large range from about 0 - 6.0 A.U. with the most populated region being between 1 and 2 AU and with many fewer comets with perihelia less than 1 AU. This may be the result of observational selection.

Everhardt (1967) as investigated the effects of observational bias on the orbital distribution of long-period comets but there has been no corresponding study of observational bias in short-period orbital distributions. Although there will be a systematic bias against comets with small perihelion distances, it is not at all clear how severe such a bias will be. It is also important to note that the orbital distribution of the parent comets is not the same as the source production function since those comets with orbits that bring them close to the Sun will produce correspondingly more meteoroids than more distant comets.

Table 4.2 Observed orbital parameters of JF_m comets

Parameter	**Mean**	**Standard deviation**
Perihelion distance	1.85	0.90
Aphelion distance	5.47	0.56
Inclination	14.2	10.0
Tisserand parameter	2.80	0.17

Our model must yield the observed $r^{-1.3}$ dependence of particle concentration on distance from the Sun and we start by constraining the apehlion distribution of the source to be identical to that of their parent Jupiter family of comets. While we consider our estimate of the aphelion distribution of the source to be fairly reliable, the perihelion distribution is unknown since besides the observational biases involved there are also the unknown effects of the variation of sublimation efficiency with age. After careful consideration we chose the following distribution function for the perihelia:

$$n(q) \propto \left\{1 - (q/2.3)^m\right\}^n (q/2.3)^{m-1} \qquad (4.1)$$

for the range $0 < q < 2.3$ AU. Not only does this distribution go to zero as it should beyond 2.3 AU, it is also extremely flexible through the choice of the parameters m and n which are yet to be determined. Since the Q and q appear to be uncorrelated, they can be

generated separately. The aphelion distances are taken to be gaussianly distributed with mean and standard deviation as given in Table 2.

With a given {m,n} we can then calculate the particle concentration, S(r), as a function of heliocentric distance, r, using

$$S(r) \propto \frac{1}{r} \sum_i \frac{1}{(Q_i + q_i)\sqrt{(r - q_i)(Q_i - r)}} \tag{4.2}$$

For this step of the calculations the orbital inclinations were not required. It is clear that since the particle concentration is seen to vary as $r^{-1.3}$, there exists an infinite set of values of m and n that will satisfy this requirement and that other constraints must be invoked to determine the values that best fit all the observations.

Zodiacal light observations show that the particle concentration increases with decreasing heliocentric distance; this seems to imply some mechanism, such as the Poynting-Robertson effect, that transports the particles towards the Sun. To include the PR effect we need to know how long the particles are likely to survive. It is generally agreed (Grün *et al*, 1985) that of the two processes active in reducing the particle population, catastrophic collisions with other meteoroids are more important than erosion resulting from collisions with much smaller particles. A detailed theory of collisional lifetimes is beyond the scope of this paper but we have adopted the following simple approximation.

First we have assumed that for these short-period particles there is no dependence of the collisional lifetimes on orbital inclination since the majority of these orbits have low inclinations. We can expect the rate collisions with particles of similar size to vary as $q / r^{1.3} a^{1.5}$. If the orbit is almost circular then q, r and a are almost equal. If the orbit is very eccentric, then the rate should not differ from this by a factor of more than 2. Close to perihelion passage the trajectory is almost semicircular with a and r being almost equal and there will be a small contribution from the remainder of the orbit. The relative size of the projectile particle in a catastrophic collision is determined by the kinetic energy available an so varies as the square of the relative speed. The relative collision speed, v_{rel}, is determined by a large number of factors most of which involve the collision geometry and we will take it as being

$$v_{rel} \propto 1/\sqrt{r} \tag{4.3}$$

The relative number of such particles depends on their mass distribution which we will take as a power law (Grün *et al*, 1985):

$$dn \propto m^{-2.34} dm \tag{4.4}$$

Combining all these factors, we find that the collision age, t_{coll}, may be expected to vary as

$$t_{coll} \propto q^{1.64}\, a^{1.5} \tag{4.4}$$

We have incorporated the Poynting-Robertson (PR) spiraling of the particles into the Sun assuming that the production rate of particles is constant. To calculate the effect of PR aging on the orbital parameters of the particles, we followed Wyatt and Whipple (1950) who give the following equations for the rate of change of semi-major axis, a and eccentricity, e:

$$\frac{da}{dt} = -\frac{\alpha(2+3e^2)}{a(1-e^2)^{3/2}} \tag{4.5}$$

and

$$\frac{de}{dt} = -\frac{5\alpha e}{2a^2(1-e^2)^{1/2}} \tag{4.6}$$

where $\alpha = 3.55 \times 10^{-8}/s\,\rho$ AU/y and s and ρ denote the radius and density of the particle in c.g.s. units. In the modeling procedure we typically work with 5×10^5 particles and follow their orbital evolution over several thousand years. Clearly direct integration of equation 10 and 11 would take unacceptably long computation times. We have therefore followed the scheme outlined by Wyatt and Whipple (1950) which we have modified by using numerical approximations for the time integrals making the calculation of the evolved orbits essentially as fast as by use of a look-up table.

It is convenient at this stage to introduce the quantity $\tau_{PR} = 1/4\alpha$, the time for a particle initially in a circular orbit a 1 AU to spiral into the Sun. For a particle of mass 10^{-4} g and density 1 g cm^{-3}, $\tau_{PR} = 2 \times 10^5$ years. It is also convenient to express the collisional lifetime in terms of τ_{PR} so our treatment is not limited to particles of a specific mass. In this generalized time unit we have

$$\tau_{coll} = f\, q^{1.64} a^{1.5} \tag{4.7}$$

where f is the ratio of the collisional to the PR lifetime of a particle in a circular orbit at *1AU*. This approach is not ideal since the probability of catastrophic collision changes as the orbit evolves. The increase in the computational complexity involved in dealing with coupling the collisional probability with the PR evolution would slow the modeling unacceptably but it is hoped that all these details can be hidden in a good choice of *f*.

We see that the orbital distribution is described by 3 parameters: *m*, *n*, and *f* and these must be determined by a comparison with observations. Up until quite recently the best large catalogue of Earth-based meteor observations was that produced by the Harvard Radio Meteor Project (HRMP) in the 60's and 70's (Sekanina, 1976). This was an extremely ambitious undertaking that has provided the most reliable source of meteor data for over three decades. It is only now that we are able to improve on the HRMP data by virtue of the present advances in electronic and computer technology. Probably the most important deficiency of the HRMP data was that it was not corrected for the biases

introduced by the initial radius effect (Greenhow and Hall, 1960). For many years there has been a marked lack of consensus as to how such corrections should be made. Recent insight (Campbell-Brown and Jones, 2003) into the physics needed to explain observations made with a unique 3-frequency radar, Canadian Meteor Orbit Radar (CMOR), has yielded a model of meteor ablation that is in good agreement with observation. We have therefore used the data from the CMOR radar together with the $r^{-1.3}$ dependence of the dust concentration determined from the zodiacal light studies to determine the unknown parameters.

Three unknown parameters require three dependent observational diagnostic quantities for their determination. The first is provided by the zodiacal light studies and the radar provided the mean speed and the mean longitude of the helion/antihelion sources. Before this could be accomplished, the geometry and biases involved in radar meteor observations need to be modeled.

5. The measured directionality of the meteoroid fluxes

In this section, our task is to transform the set of orbits we have generated into meteoroid fluxes. It is usually assumed that the particle density distribution is separable into radial and latitudinal parts. For the trivial case of an isotropic distribution of the orientation of the orbital planes there is no latitudinal variation but in general the latitudinal variation can be expressed in the form of an integral (Kessler, 1981; Steel and Elford, 1986). We will limit our discussion to the particle concentration in the ecliptic plane since although our treatment can be extended to the out-of-the-ecliptic case; we consider it a needless complication at this stage.

For each particle we will have to calculate the probability of it being at a given distance from the Sun as well as its velocity. The first of these is easily accomplished using the theory from the preceding sections but the determination of the velocity requires that we know the inclination of the orbit of the particle. We will assume that inclination distribution of the meteoroids is similar to that of the JF_m comets since it is difficult to imagine a mechanism that would change significantly the distribution of inclinations of particles in this size range after they are released from their parent comets. Figure 6 shows the distribution of inclinations of the JF_m comet population. We fitted the cometary inclination data with the distribution function

$$n_{pop}(i) \propto \sin(i)\, e^{-(i/15.9)^2} \tag{5.1}$$

that is well suited to the spherical geometry. Because of geometric considerations, only particles with orbital planes containing the Sun-Earth line can intersect with the Earth. This limits the intersecting orbits to that have poles lying on a great circle whose plane is perpendicular to the Sun-Earth line as shown in figure 5.1 below. The distribution of inclinations for these orbits is therefore different to that for the total population of particles and a little consideration shows that whereas the inclination distribution for the whole set of JF_m particles is given by equation 13, that of the Earth-intersecting particles is given by

$$n_{Earth\ \ intersecting}(i) \propto e^{-(i/15.9)^2} \tag{5.2}$$

We now need some expressions to allow us to calculate the velocity, $\vec{v}$, of a given particle. Its speed, v, in units of the Earth's speed, is given by

$$v = \sqrt{2/r - 1/a} \tag{5.3}$$

and it is easily shown that at any point in the orbit, if the angle between the velocity vector and the radius vector is ψ, then

$$\psi = \arcsin(a^2(1-e^2)\ /\ r(2a-r)) \tag{5.4}$$

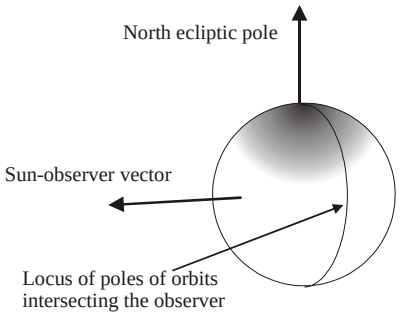

Figure 5.1 Although the poles of the orbits are distributed over the shaded area of the celestial sphere, only those that fall on the great circle perpendicular to the Sun-observer line can intersect with the observer.

with the particle either approaching or receding from the Sun. The velocity vector of a given particle is given by

$$\vec{v} = v\begin{pmatrix} \pm\cos(\psi) \\ \sin(\psi)\cos(i) \\ \pm\sin(\psi)\sin(i) \end{pmatrix} \tag{5.5}$$

where the angles are as shown in figure 5.2 below.

The weight, w_k, for the k^{th} simulated particle allows for the probability that it will be found at a given distance from the Sun is given by

$$w_k = \frac{N(Q_k, q_k)}{r(Q_k + q_k)\sqrt{(r-q_k)(Q_k - r)}} \tag{5.6}$$

as in equation 1.1. We note that w_k is also a measure of the contribution to the total particle concentration by a given particle.

We are usually interested in the particle fluxes as would be seen from a moving platform - e.g. the Earth or a space probe and so the next step is to calculate the velocities of the simulated particles as would be seen in this moving frame of reference. If the velocity of the observation platform is $\vec{v}_p$, the apparent velocity, $\vec{v}_a$, is given by

$$\vec{v}_a = \vec{v} - \vec{v}_p \tag{5.7}$$

When speaking of a particle flux we must specify what determines the smallest particle that can be included. We often speak of flux above a given mass or momentum limit. Suppose we want the flux above a certain parameter, *z*, which varies with mass and velocity as

$$z \propto m\, v_a^{\gamma} \tag{5.8}$$

For mass flux, i.e. flux of particles above a given mass limit, $\gamma = 0$; for momentum flux $\gamma = 1$, and according to Verniani (1965) for the flux of radar meteors (ionization flux) $\gamma = 4$ although Jones (1997) has suggested a somewhat weaker dependence. Usually $\gamma \geq 0$, so that for a given value of *z*, higher values of v_a will correspond to smaller masses.

The number of sporadic meteoroids per unit volume, dN_v in the mass range *m* to *m* + *dm* is usually taken to be well described by a power law:

$$dN_v \propto m^{-s} dm \tag{5.9}$$

with s is close to 2.34 (Whipple, 1967; Grün *et al,* 1985) so that the number of particles per unit volume with mass greater than the smallest detectable mass m_0 is proportional to m_0^{1-s}. The cumulative flux, Φ_c, of particles with $z > z_0$ is then given by

$$\Phi_c \propto \sum_k w_k \; v_{a,k}^{\gamma(s-1)+1} \tag{5.10}$$

We can also calculate the speed distribution, *n(V),* for the particles impacting the observation platform using

$$n(V) \propto \sum_k w_k \; v_{a,k}^{\gamma(s-1)+1} \; h(v_{a,k}, V) \tag{5.11}$$

where $h(v,V)$ is a binning function defined such that

$$h(v,V) = \begin{cases} 1 & |v - V| < \varepsilon_V \\ 0 & otherwise \end{cases} \qquad (5.12)$$

.

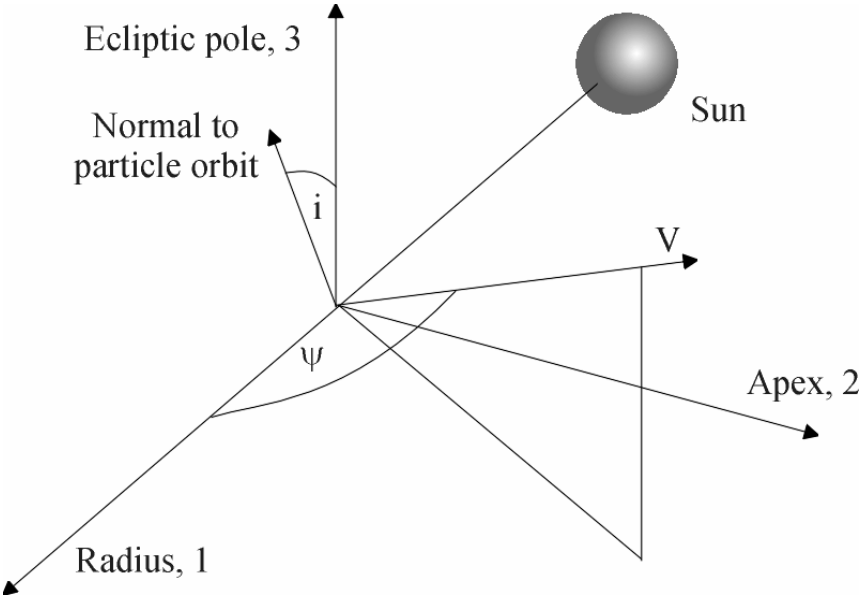

Figure 5.2. Geometry of trajectory at point of observation. ψ is the angle between the trajectory at the observer and the Sun-observer line.

6. Predicted short-period meteor activity at Earth's orbit

We now discuss the results of the fitting of the various parameters of the short-period comet source to observations the radiant and speed distributions of sporadic meteors. Table 6.1 summarizes the measured characteristics of the helion/antihelion sources according to Brown (1994) and Jones and Brown (1993) from an analysis of radar meteor data from the IAUMDC (Lindblad, 1987) together with the very recent values determined using the UWO meteor radar (CMOR) after correction has been made for the initial radius effect.

.

Table 6.3 Radar determinations of helion/antihelion characteristics

	HRMP	**CMOR (2003)**
Helion long.	341 – 345 deg	338 deg
Antihelion long.	193 – 201 deg	202 deg
$\langle V_g \rangle$	31.7 km/s	34.4 km/s

The CMOR data must be considered superior to that from the HRMP because of the initial radius correction. The HRMP determined speeds using Fresnel oscillations of the echoes which are evident only for non-fragmenting meteoroids so that this catalogue applies primarily only to that small fraction of the meteoroid population that does not fragment during ablation in the Earth's atmosphere. An additional cause for concern is that speed determinations from the Fresnel oscillation are error prone since the amplitude of the oscillations is small compared with the amplitude of the echo. The CMOR entries in Table 6.1 are the final result after three following corrections had been made to the mean observed speed. The first was for the initial radius effect which gave a corrected mean speed of 33.0 km/s. The empirical formula due to Baggaley *et al* (1994):

$$V_\infty^2 = V_o^2 + 0.81 V_o^{1.6} \tag{6.1}$$

was then applied to allow for deceleration in the Earth's atmosphere and lastly the increase in speed due to the Earth's gravity was removed using the standard formula

$$V_g^2 = V_\infty^2 - 125 \tag{6.2}$$

We have determined the values of the parameters m, n, and f that provide the best fit with the CMOR data. They are: *m = 10; n = 1.69 and f = 0.3*. A word of caution is probably in order at this point: the CMOR (2003) data are our first results using this new system and both the speed and orbital determinations can certainly be improved upon. Figures 6.1 and 6.2 show the model predictions for radiant and speed distribution of meteors from the short-period source for ionization (radar) and figures 6.3 and 6.4 show similar plots for mass weighting.

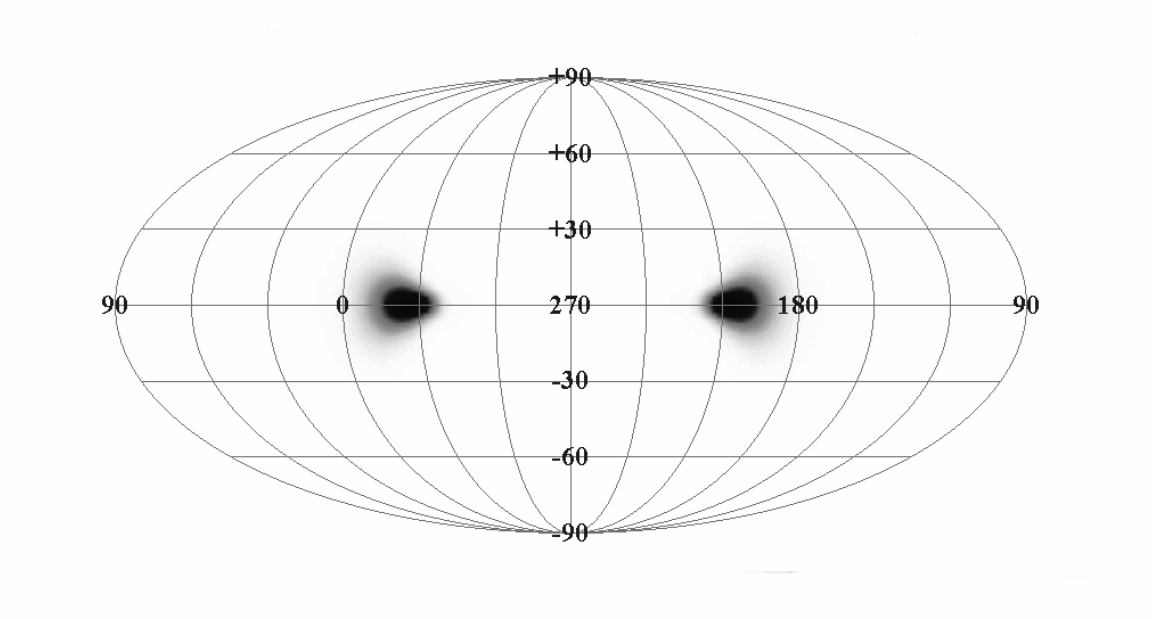

Figure 6.1. Predicted radiant distribution of meteoroids from the short-period comet source as would be observed from an Earth-based meteor radar.

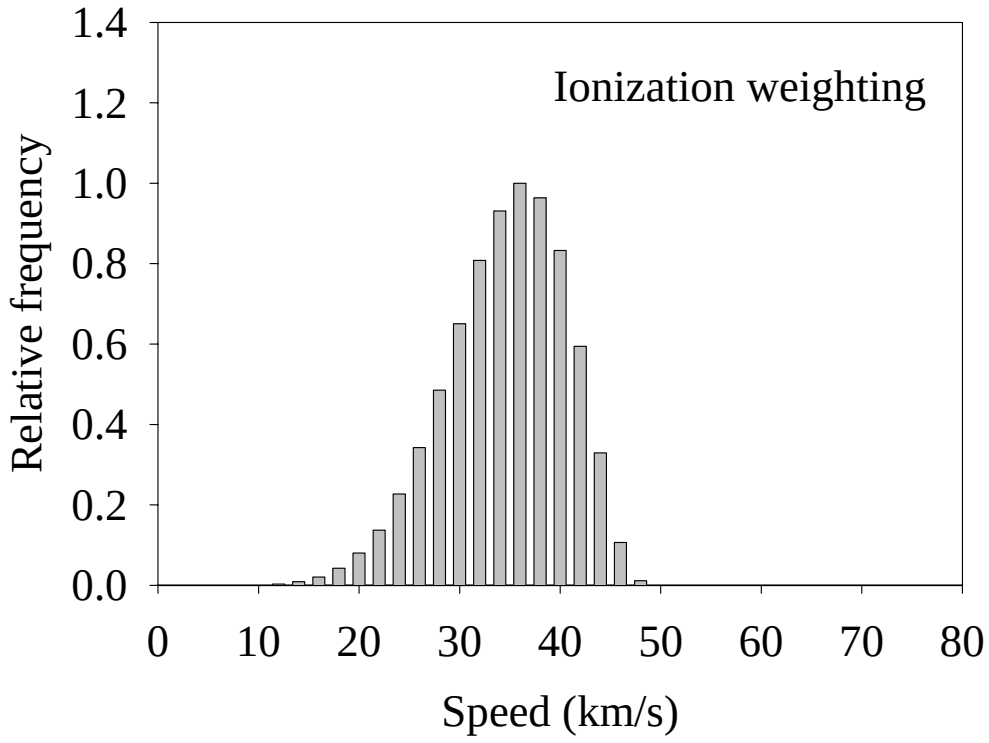

Figure 6.2 Predicted speed distribution of meteoroids from the short-period comet source as would be observed from an Earth-based meteor radar. The mean speed is 34.5 km/s.

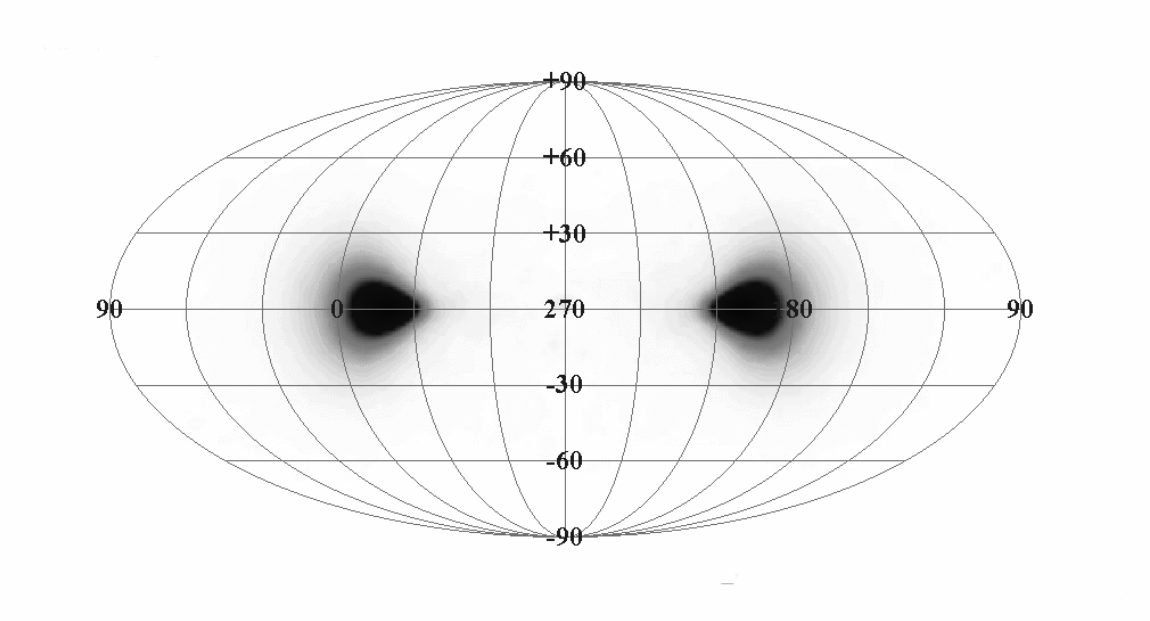

Figure 6.3. Predicted radiant distribution of meteoroids from the short-period comet source as would be observed from an Earth-based mass-limited meteor

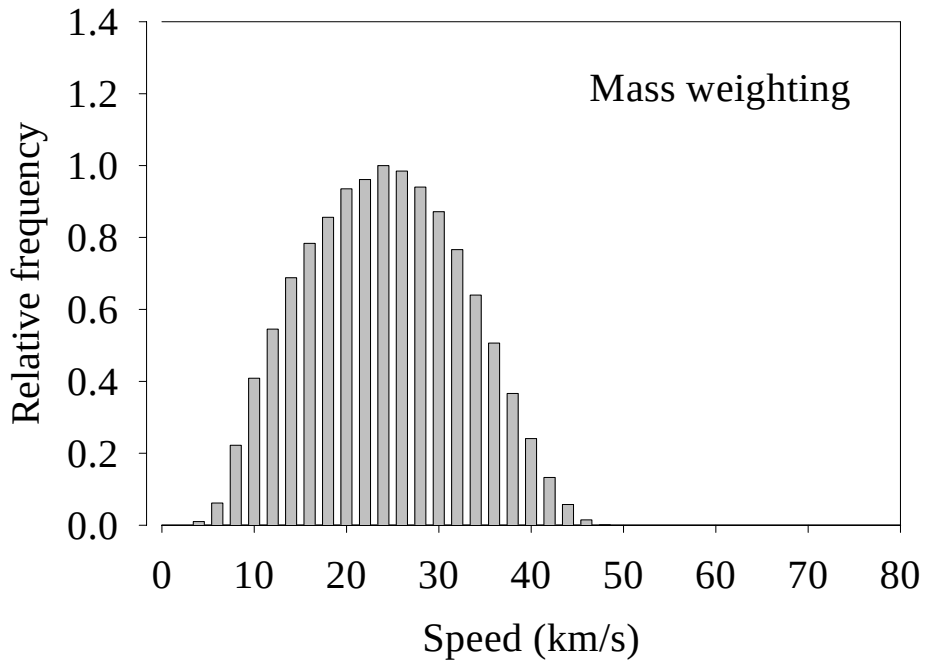

Figure 6.4 Predicted speed distribution of meteoroids from the short-period comet source as would be observed from an Earth-based mass-limited meteoroid detector. The mean speed is 24.1 km/s

Before proceeding further it is probably appropriate to make some remarks on the above predictions. Probably the most prominent feature of the model predictions is the high mean speed for the mass-limited case – 24.1 km/s as compared with the usually accepted value of about 20 km/s deduced from the HRMP. Certainly the HRMP data were biased towards lower speeds since no correction was made for the initial radius effect which causes higher speed meteors to be missed because of the increased attenuation at greater heights. Measurement errors in the speeds also have the same effect since to obtain the mass-limited speed distribution for the radar data it is usually assumed that the ionization goes as some high power of the speed such as v^4. If the observed speed distribution has been broadened by measurement error, this results in a decrease in the apparent average speed of the mass-limited speed distribution. This is easily seen when we consider the case when all the meteoroids have the same speed which will yield the same mean speed independent of whether the detector is mass-limited or ionization-limited.

Measurement errors in the speed errors introduced uncertainties in the HRMP trajectory determinations that will increase the apparent size of the helion and antihelion sources. Typically the radius of these sources deduced from the HRMP observations is of the order of 15 deg and this measurement error could well explain the discrepancy between out predicted and the HRMP–derived source radii. We hope to settle this question in the near future using the high-precision interferometer of CMOR that does not involve error-prone time-of-flight measurements.

Figure 6.5 shows the predicted dependence of concentration of particles originating from the short-period source as a function of heliocentric distance. The rapid decrease in the particle concentration beyond 5 AU is clearly a consequence of the clustering of the aphelia in this region. The agreement with the $1/r^{1.3}$ dependence from the zodiacal light studies is good but it is evident that there are some slight departures from a power law in the region 0.3 to 1.0 AU. The model predicts that the particle concentration does not continue to increase at small heliocentric distances and this is probably the result of the collisional loss of particles.

We also present in Figure 6.6, the fitted dependence of source strength as a function of perihelion distance.

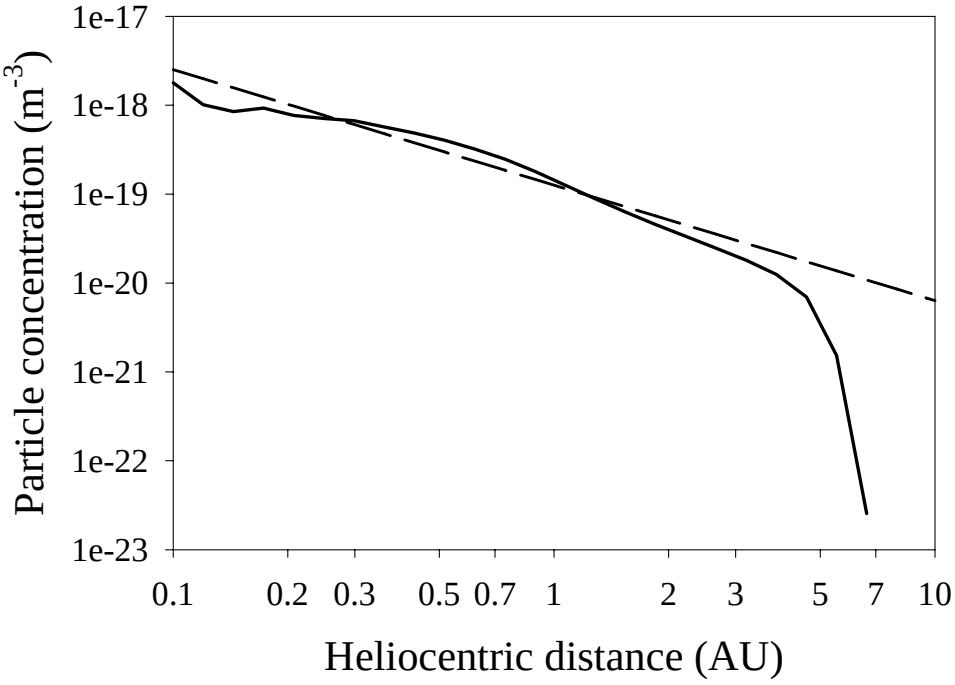

Figure 6.5 Predicted concentration of particles of mass greater than 1 g from the short-period source. The dashed line represents the $1/r^{1.3}$ dependence based on observations covering the range 0.3 to 1.0 AU

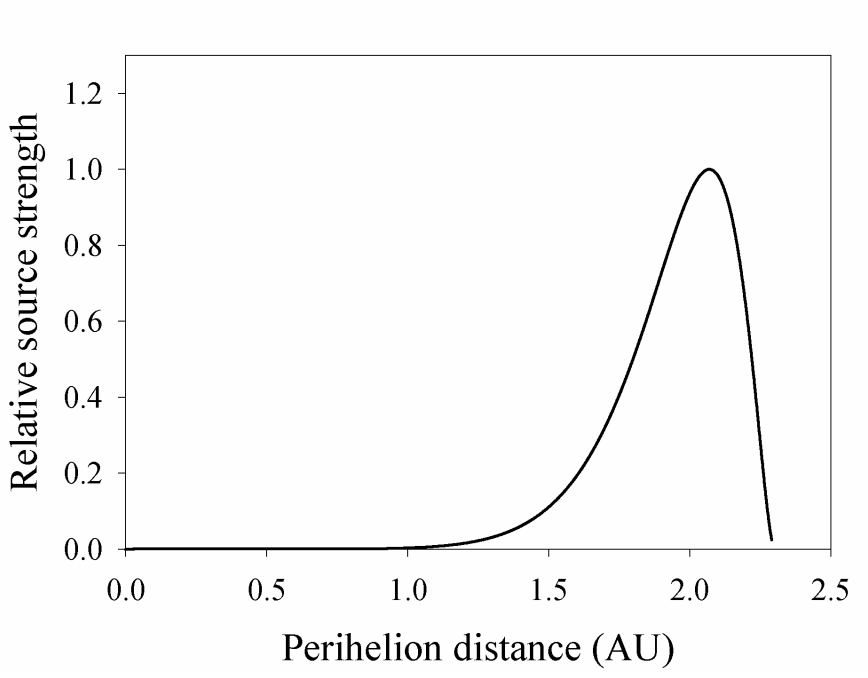

Figure 6.6 Fitted strength of short-period source as a function of perihelion distance.

7. The long-period comet source.

We will assume that the apex source is the result of the disintegration of long-period comets with perihelia closer than 2.3 AU. It is well established that the poles of these orbits are essentially uniformly distributed over the celestial sphere, according to observations with the CMOR system. After correction for initial radius effects, the Earth's gravity and atmospheric deceleration, we find the mean speed for these "apex" meteoroids is about 63.6 km/s. The other prominent feature is that the apex source is observed to be split into northern and southern components that are about $\pm 21^{o}$ from the ecliptic. From previous studies we know that the space density of these high speed meteors is a small fraction of that due to the short-period comet source and so we know little of the variation of their concentration with heliocentric distance. Thus, whereas we were able to fit a three-parameter model for the short period source, for the long-period source we can only fit a two-parameter model.

Because the orbits of long-period comets are so extended, the distribution of the dust they produce is dominated in the inner Solar System by the distribution of their perihelia. As mentioned earlier Everhardt (1967) has studied the effects of observational bias on the orbital distribution of long-period comets and has proposed a likely distribution but the observations are not comprehensive enough to define the distribution of perihelia well. The source distribution will also be dependent on the degree of sublimation and its variation with orbital parameters. We therefore propose a one-parameter distribution of perihelia that we will try to fit to the observational data:

$$n(q) \propto \left\{1-(q/2.3)^{m}\right\}(q/2.3)^{m-1} \tag{7.1}$$

From Marsden's Catalogue of Cometary Orbits (1989) we find that the inverse semi-major axis, b = 1/a, is distributed approximately exponentially:

$$n(b) \propto e^{-b/129} \tag{7.2}$$

Since the orbital poles are distributed isotropically, the distribution of inclinations will be uniform between 0 and 180^{o} because the geometry limits the accessible orbits to those with poles lying on a great circle perpendicular to the Sun-observer line.

Finally we incorporate collisions in much the same way as for short-period comets, except that in this case we consider the dependence on inclination. Since the dust from the short-period comets resides close to the ecliptic, it will be with these particles that the majority of collisions occur. Thus long-period particles with low inclination orbits will be most likely to collide with the short-period particles in the ecliptic disc. As with the short-period comet source, we the collision lifetime was characterized by the parameter *f* as in equation 4.7. In this case there is an additional factor to allow for the orbital inclination dependence so that those particles in retrograde orbits close to the ecliptic will have much shorter lifetimes than those with pro-grade orbits because of the difference in their relative impact speeds.

$$\tau_{coll} = f\ q^{1.64}\ a^{1.5}\ e^{\frac{1}{2}\left(\frac{i-180}{11.2}\right)^2} \qquad (7.3)$$

Our best fit of the model to the observations yields $m \approx 1$ and $f \approx 0.002$. Of these, m is the most uncertain since the observed parameters depend only weakly on m. On the other hand, the value of f determines the separation of the North and South Apex sources as might have been anticipated.

The mean speed corrected for initial radius of North Apex meteors is 59.8 km/s. This yields a geocentric speed of 63.3 km/s after allowing for the Earth's gravity and atmospheric deceleration. Although we expended considerable effort we were unable to find values of m and f that would yield a mean speed above 59.1 km/s. The reason for this is not clear but may lie in an overestimate for the correction (about 3 km/s) for atmospheric deceleration. It is also possible that our assumed variation of ionization efficiency with speed is incorrect and it may be that the dependence is stronger than v^4. Indeed there has been little experimental work done on this problem for many years - probably because it is so difficult to accelerate particles in the laboratory to speeds greater than about 10 km/s and it is encouraging that the agreement is as good as it is.

Whatever the reason, we found that the predicted mean speed of meteoroids from the long-period comets is remarkably insensitive to the forms of the both the perihelion and semi-major axis distributions. We therefore considered that, in the absence of any good diagnostic quantities such as mean speed, it is probably best to go with Everhardt's estimate of the perihelion distribution modified for sublimation.

By using the CMOR observations to calibrate the predicted fluxes, we have determined how the concentration of particles varies with heliocentric distance and this is shown in figure 7.5 together with the corresponding results for the short-period source. It is evident that in the inner Solar System as far as 5 AU the particles from the short-period source are far more numerous than those from the long-period source but beyond 7 AU meteoroids shed from long-period comets dominate.

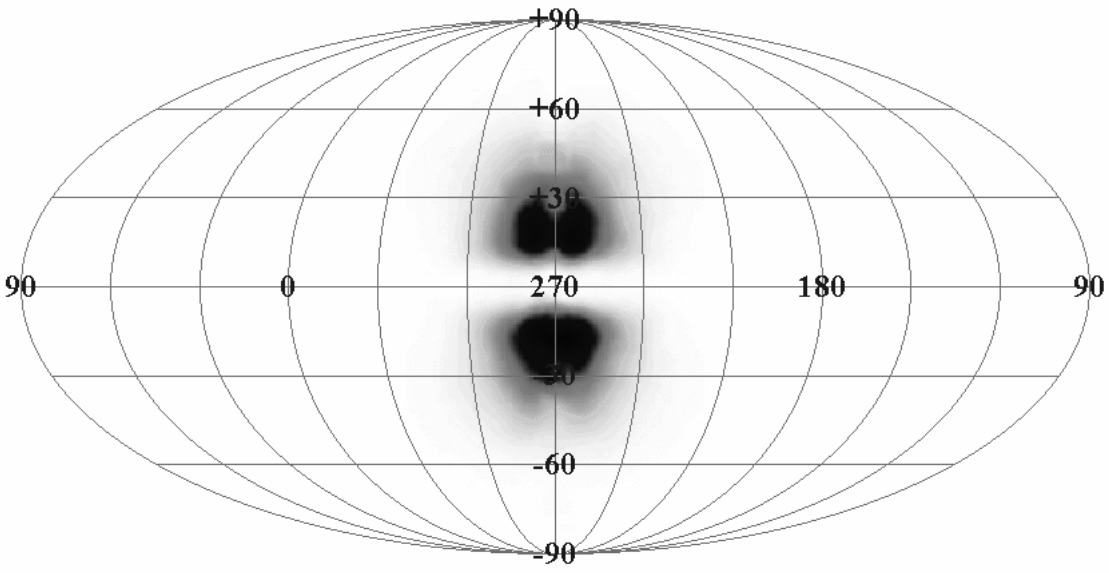

Figure 7.1 Predicted radiant distribution of meteoroids from the long-period comet source as would be observed from an Earth-based meteor radar.

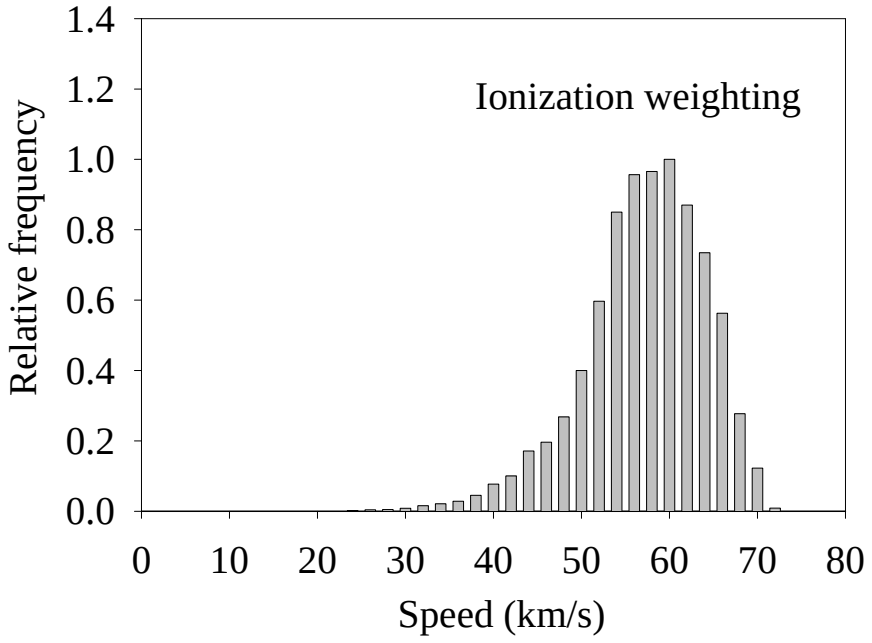

Figure 7.2 Predicted speed distribution of meteoroids from the long-period comet source as would be observed from an Earth-based meteor radar. The mean speed is 57.2 km/s. The solid line shows the measured speed distribution.

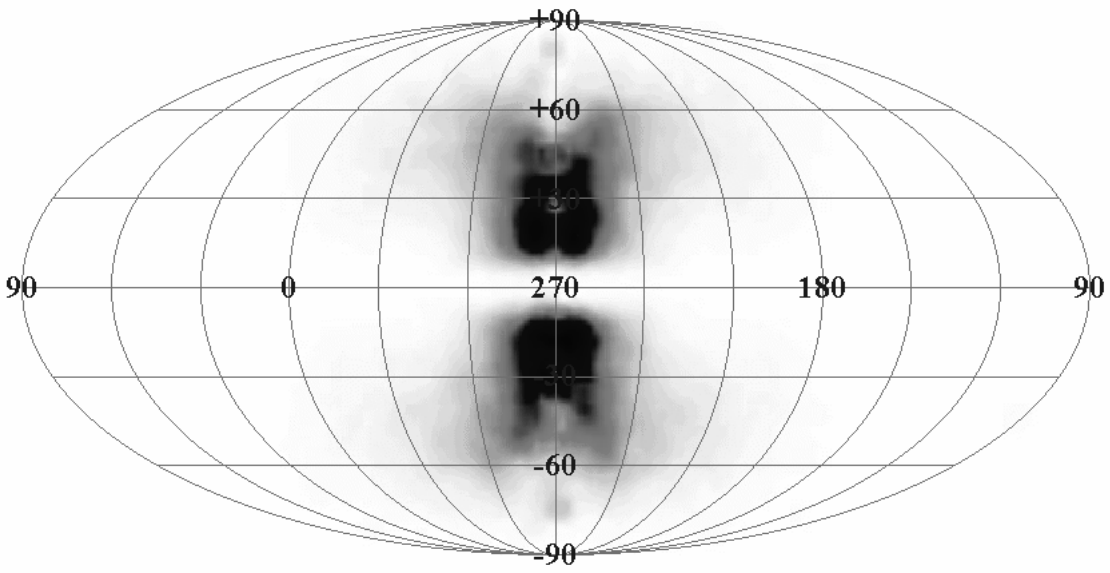

Figure 7.3 Predicted radiant distribution of meteoroids from the long-period comet source as would be observed from an Earth-based mass-limited meteoroid detector.

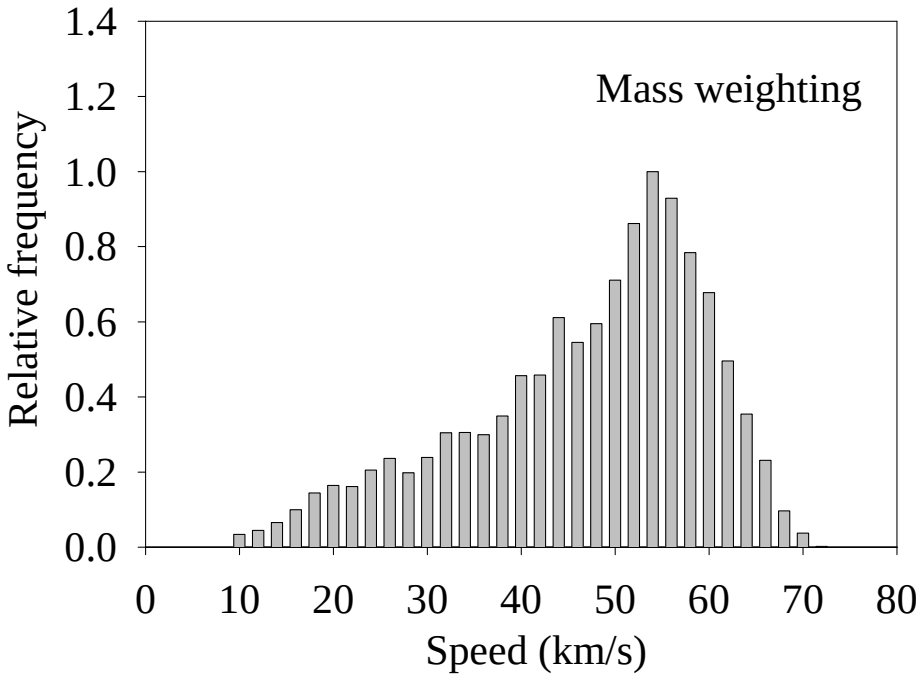

Figure 7.4 Predicted speed distribution of meteoroids from the long-period comet source as would be observed from an Earth-based mass-limited meteoroid detector. The mean speed is 47.0 km/s

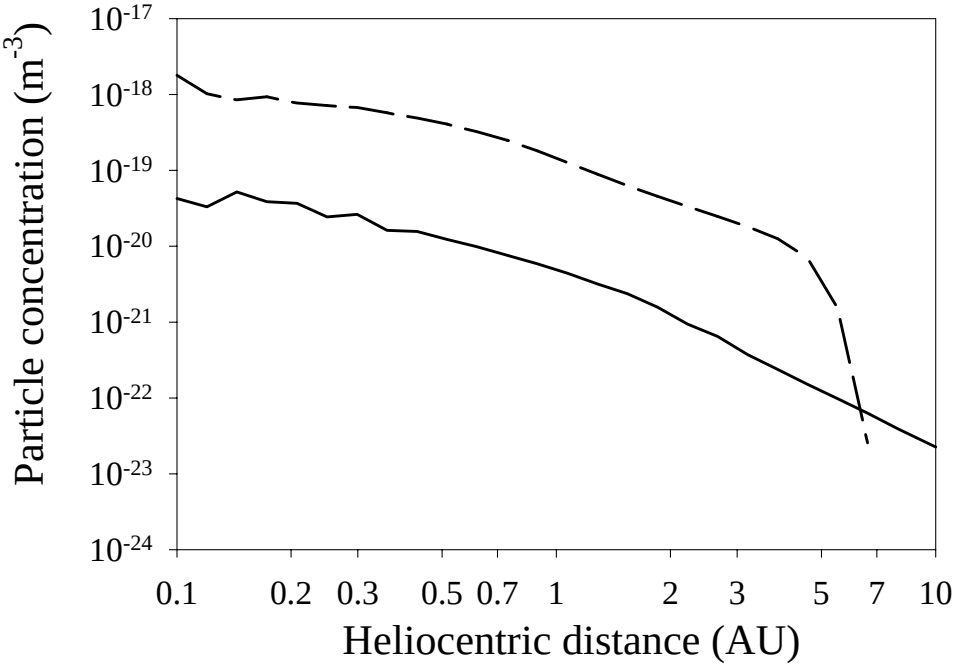

Figure 7.5 Concentration of particles from the long-period source (solid line) and short-period source (dashed line) versus heliocentric distance.

8. The toroidal source.

The toroidal source close to latitude 60^o and longitude 0^o has remained an enigma since its discovery by Stohl (1968). From an analysis of the HRMP observations Jones and Brown (1993) found that meteoroids from the source have a mean speed of about 36 km/s. On the other hand Campbell-Brown and Jones (2003) after applying the initial radius correction find a mean speed of 41.3 km/s.

It is clear that the inclination distribution of these meteoroids is not isotropic since this would produce radiants in the direction of the Apex similar to what is observed from the long-period source. We must conclude that these are not from long-period comets and are therefore somehow associated with short-period comets. We will tentatively assign them to the Halley group of comets which have periods in the range 20 – 200 y and distribution of inclinations which is several times greater than for those from the Jupiter family.

For this class of meteors we have very little information to base our model on. Because the inclinations of the observed toroidal meteors are so high, they have spent most of their lives out of the ecliptic and therefore been much less suffered from collisions in the ecliptic dust disc. We will therefore start by ignoring collisions. We have no idea what

the effects of observational selection are and we will therefore assume the perihelia are distributed as indicated by equation 7.1. We will take the inverse semi-major axis to be uniformly distributed between 0.0292 and 0.136 AU^{-1} corresponding to the range in periods mentioned above. In the absence of anything better, we take the inclinations to be Gaussianly distributed. We have tried to fit a model with the two parameters *m* (in equation 7.1) and the r.m.s. width of the inclination distribution. The parameter *m* seems to control the longitudinal extent of the radiant activity but in a way that is not easy to quantify but *m = 4* seems to be the best choice based on visual inspection.

The mean predicted speed, $<v>$, seems to be dependent almost entirely on the r.m.s. inclination spread, σ_i,:

$$< v > = 11.5 \quad + \quad 0.85\sigma_i \tag{8.1}$$

The HRMP observations would suggest that $\sigma_i = 29^o$, while the CMOR data is consistent with $\sigma_i = 35^o$, both of which are in fairly good agreement with the corresponding value for the Halley family of comets of close to 30^o. The mean latitude of the radiant activity is also dependent on the scatter of inclinations with HRMP data yielding a slightly better agreement with the observed value than the CMOR observations. At this stage we can only conclude that the model is substantially correct but the degree of agreement between theory and observation depends on the many assumptions that have been made. For example we have assumed the inclination distribution to be Gaussian but we could have chosen many others such as a Lorentzian and improving the fit is a task for future work.

The results of this fitting procedure are shown in figures 8.1 – 8.4. The form of the radiant activity is the result of the orbits being circularized by the PR effect so that those orbits with small inclinations will be travelling with almost the same velocity as the Earth. Such meteoroids will have very small velocities relative to the Earth and will consequently produce low fluxes and be difficult to observe. The relative velocity increases with increasing inclination but at the same time the number of obits with these higher inclinations decrease. The latitudinal maximum of the radiant distribution is therefore determined by these competing effects.

Figures 8.1 to 8.4 show the predicted radiant and speed distributions for ionization and mass weighting while figure 8.5 shows how the space density due to the toroidal source varies with heliocentric distance. It is clear that within Jupiter's orbit, particles from the short-period source dominate while immediately beyond this region particles from the toroidal source are more numerous than those shed from long-period comets.

In figure 8.6 we show the predicted flux of radio meteors at 1 AU versus the geocentric speed. Figure 8.7 shows a similar plot of predicted flux versus geocentric speed but this time it is for a mass-limited detector. We should note that previous attempts to determine this distribution have used the HRMP data and have ignored the errors in the measured speeds, which has the effect of increasing the apparent fraction of low speed meteors.

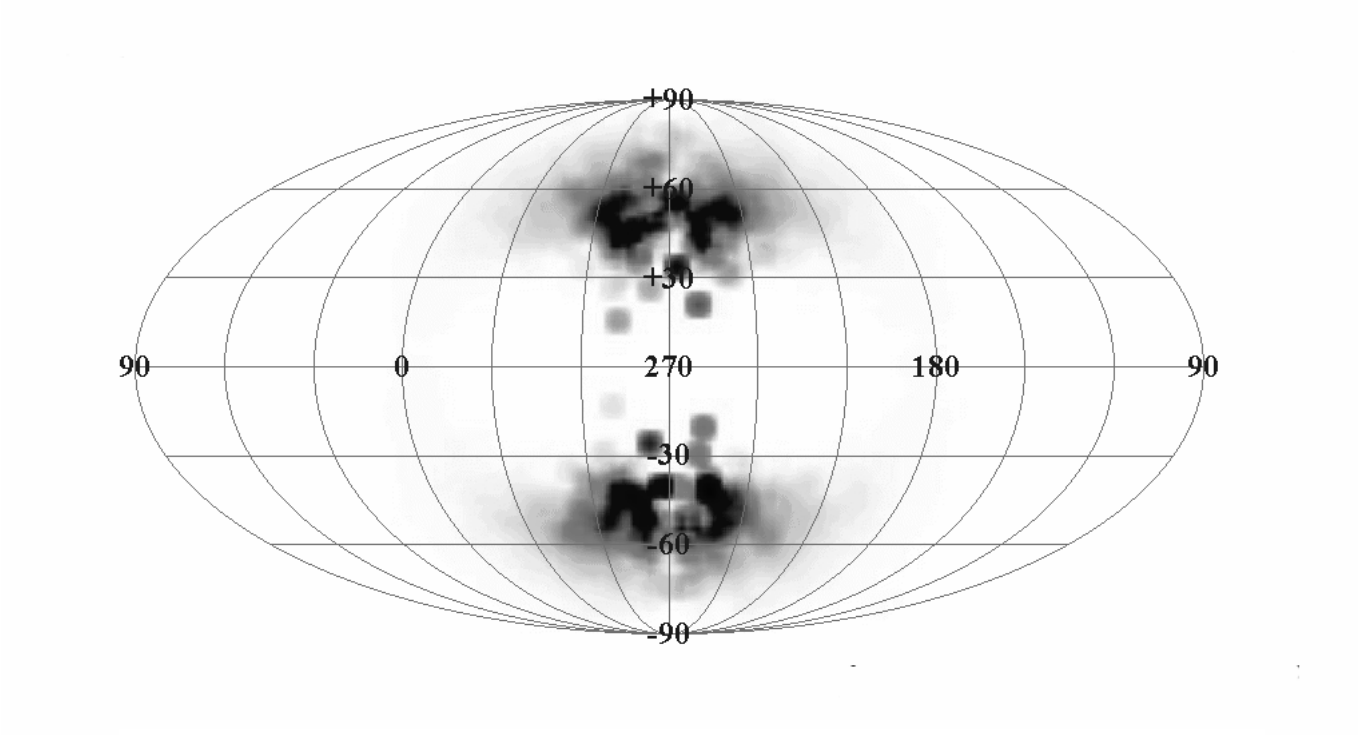

Figure 8.1 Predicted radiant distribution of meteoroids from the Toroidal Source as would be observed from an Earth-based meteor radar.

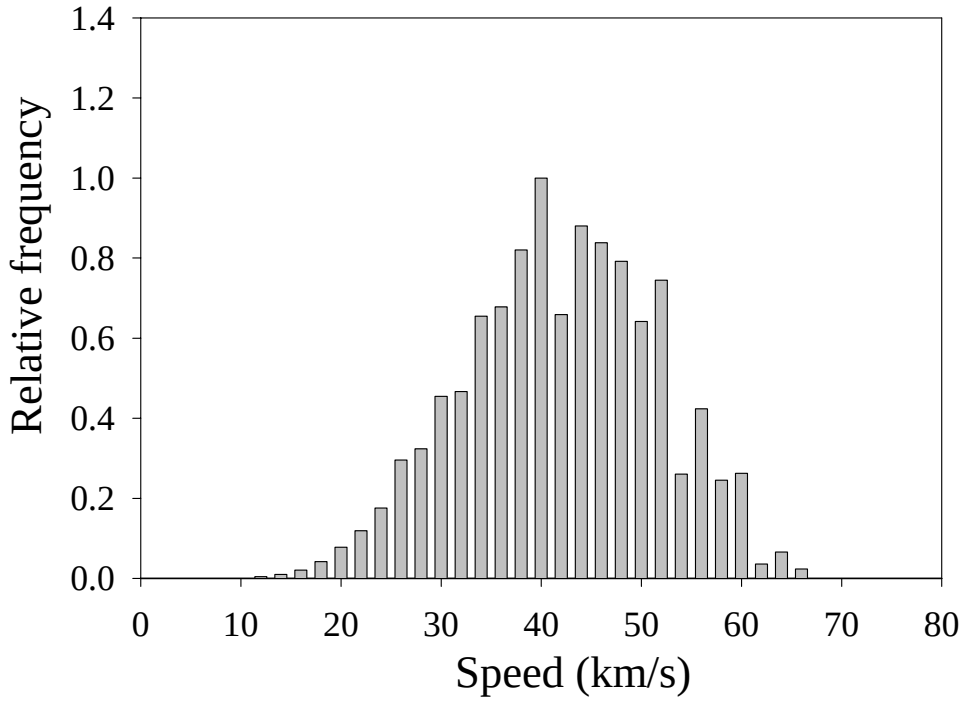

Figure 8.2 Predicted speed distribution of meteoroids from the Toroidal Source as would be observed from an Earth-based meteor radar. The mean speed is 42.0 km/s.

Figure 8.3 Predicted radiant distribution of meteoroids from the Toroidal Source as would be observed from an Earth-based mass-limited meteoroid detector.

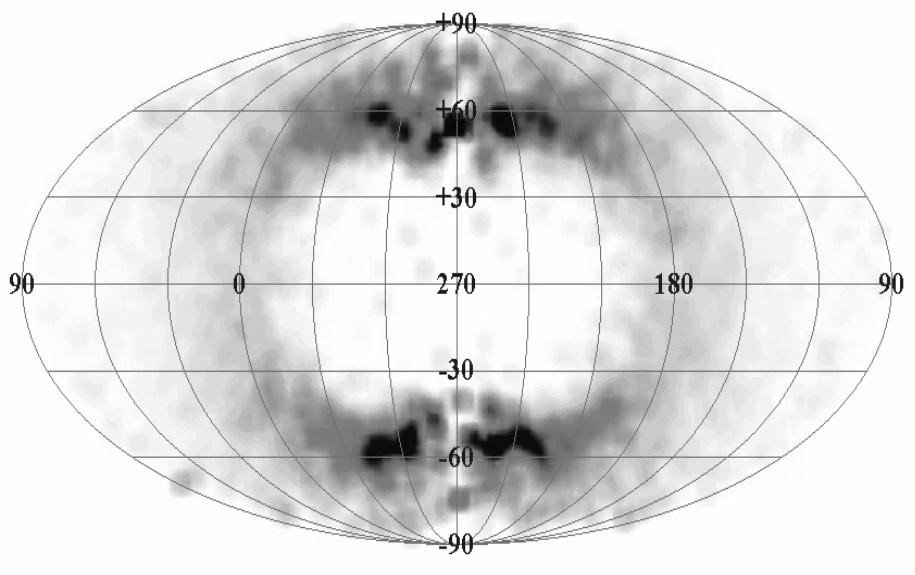

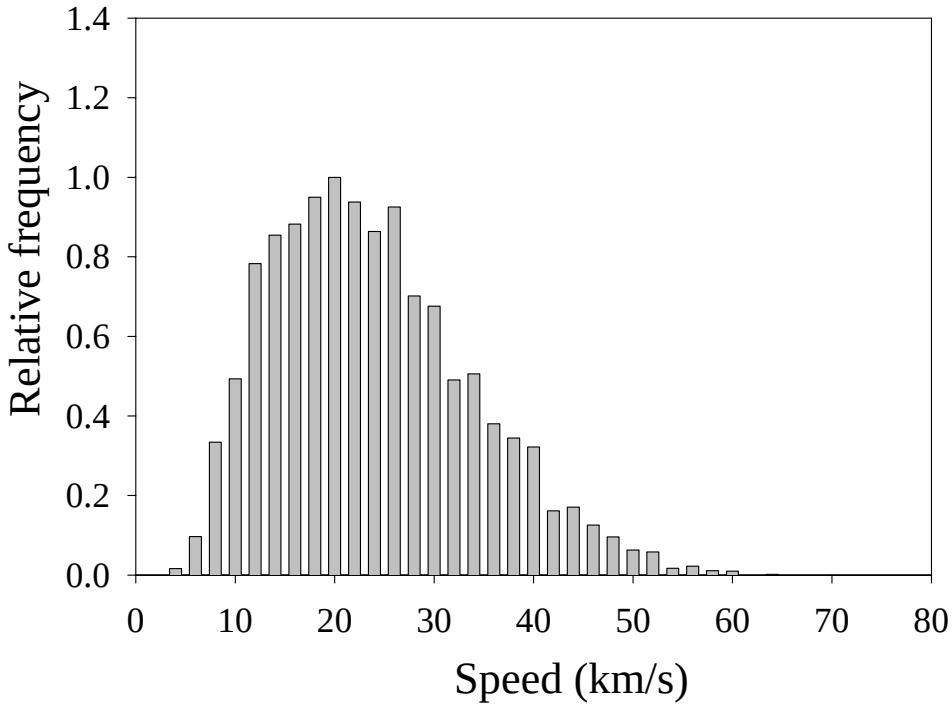

Figure 8.4 Predicted speed distribution of meteoroids from the Toroidal Source as would be observed from an Earth-based mass-limited meteoroid detector. The mean speed is 23.8 km/s

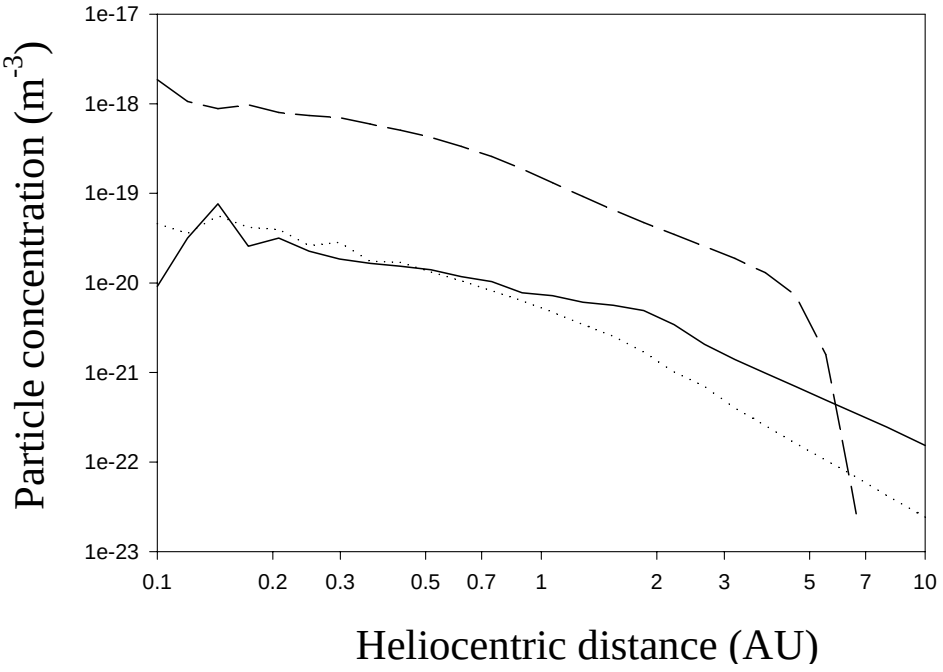

Figure 8.5 Predicted concentration of particles of mass greater than 1 g at 1 AU. Solid line: Toroidal source; dashed line: short-period source; dotted line long-period source.

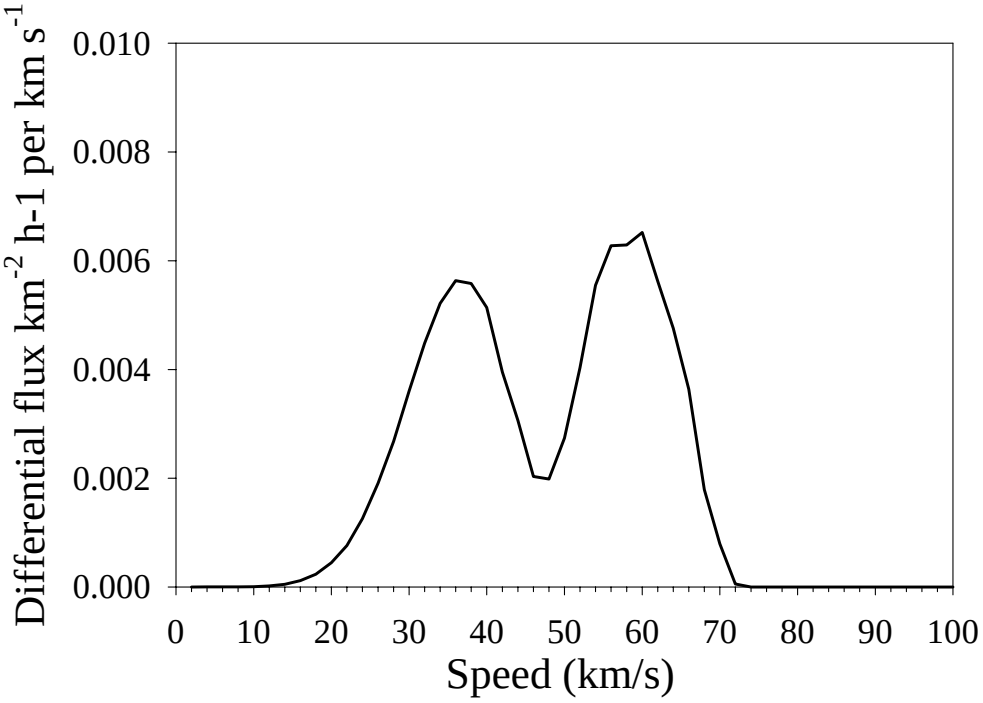

Figure 8.6 Predicted differential flux of meteors of radio magnitude <+6.5 as observed from an Earth-based platform.

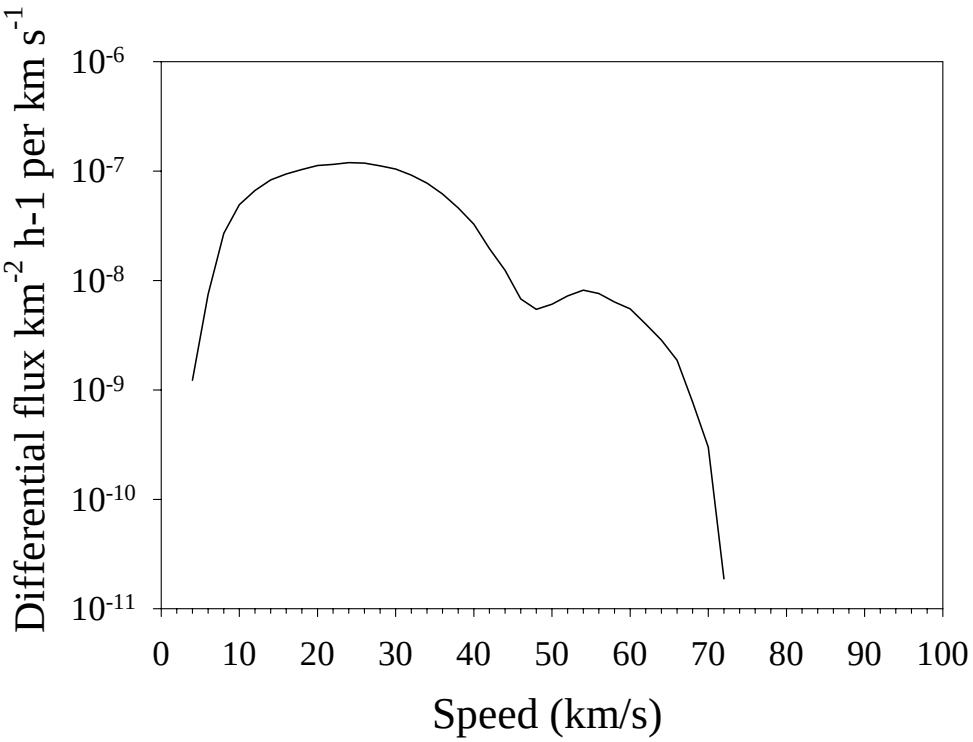

Figure 8.7 Predicted differential flux of meteors of mass > 1 g as observed from an Earth-based platform.

9. The asteroidal source

It has long been assumed that meteoroids have their origins in both comets and asteroids but how one might distinguish one variety from the other is not obvious. Although a cometary origin seems to explain all the characteristics we observe in sporadic meteors we should also address the question of what the observed characteristics of asteroidal meteors are expected to be.

J.C. Liou has kindly provided me with a compilation of the observations of 25μ asteroidal particles and these are shown in figures 9.1 – 9.3. Since we have no observational constraints from radar meteor observations, there are no adjustable parameters. In particular we have made no allowance for depletion of the asteroidal population resulting from inter-particle collisions. This should not be make much difference to the final results since these orbits have low eccentricities to start with and the PR effect only makes them more circular. Because of the near circularity of the orbits, only orbits with semi-major axes close to 1 AU will be observed from Earth and these will be much the same whatever their age.

To model the asteroidal orbits we used the Monte-Carlo method for the generation of semi-major axes. We used a fifth-order polynomial approximation for the normalized distribution function of the semi-major axes:

$$n(a) = \sum_{k=0}^{5} c_k \; a^{k} \tag{9.1}$$

where a is limited to the range 2.13 to 3.6 AU and where c is given by

$$c = \begin{pmatrix} -653.25 \\ 1182.52 \\ -844.97 \\ 297.49 \\ -51.53 \\ 3.51 \end{pmatrix} \tag{9.2}$$

We found that the distribution of eccentricity, ecc, is well described by a Weibull distribution:

$$n(ecc) \quad \propto e^{-(ecc/0.158)^{2.24}} (ecc/1.58)^{1.24} \tag{9.3}$$

For the inclination distribution we used a double Gaussian:

$$n(i) \propto 8.57\, e^{-(i/2.57)^2} + 2.57\, e^{-(i/8.57)^2} \tag{9.4}$$

Having generated a set of initial orbits we then let then calculated the equilibrium distribution of orbits assuming the source strength to be constant and the only depletion mechanism to be the PR effect. We then "observed" these particles from a point at *1 AU* from the Sun moving in an Earth-like orbit. The results of these calculations are shown in Figures 9.4 – 9.7.

The most remarkable feature is that the observed asteroidal meteoroids are predicted to have inclinations close to $\pm 90^{o}$. A little thought shows that this is because the majority of the particles are moving with almost the same velocity as the Earth so that their relative speeds and thus fluxes are very small. This is predominantly the case in the apex direction. The relative velocity increases for greater inclinations but because the inclination distribution is fairly narrow, the relative speed cannot be much greater than a few km/s and a little consideration of the geometry involved shows that the relative velocities must be almost perpendicular to the apex direction. The v^4 dependence of ionization efficiency on speed emphasizes the high speed tail of the speed distribution for radar meteors so that their mean speed is somewhat higher than for those observed with a mass-limited detector.

The fact that we cannot observe these particles does not mean that they are absent – they are just moving with almost the same orbital velocity as the Earth. Because their relative velocity is so small the flux of these particles is also correspondingly low.

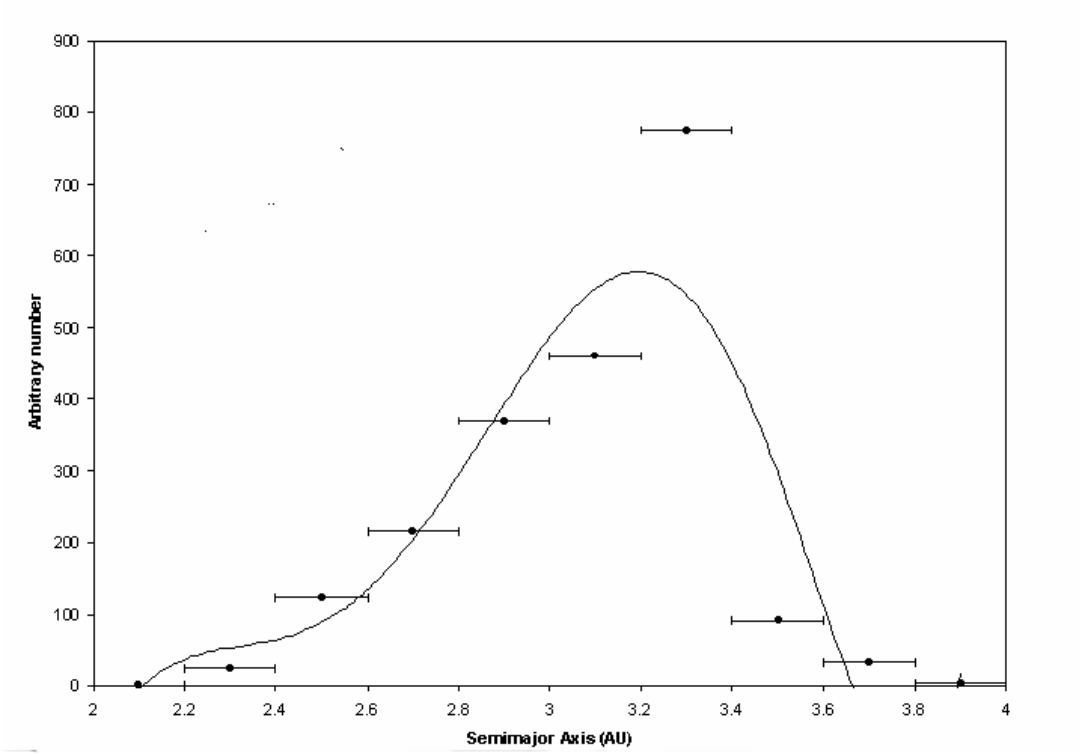

Figure 9.1 Distribution of semi-major axes of 25μ asteroidal particles

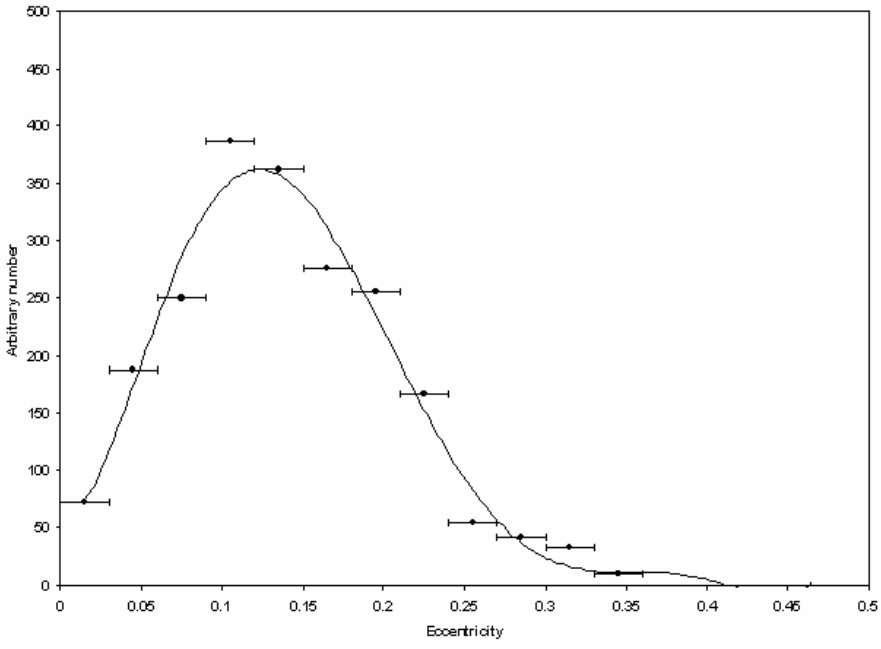

Figure 9.2 Distribution of eccentricities of 25μ asteroidal particles

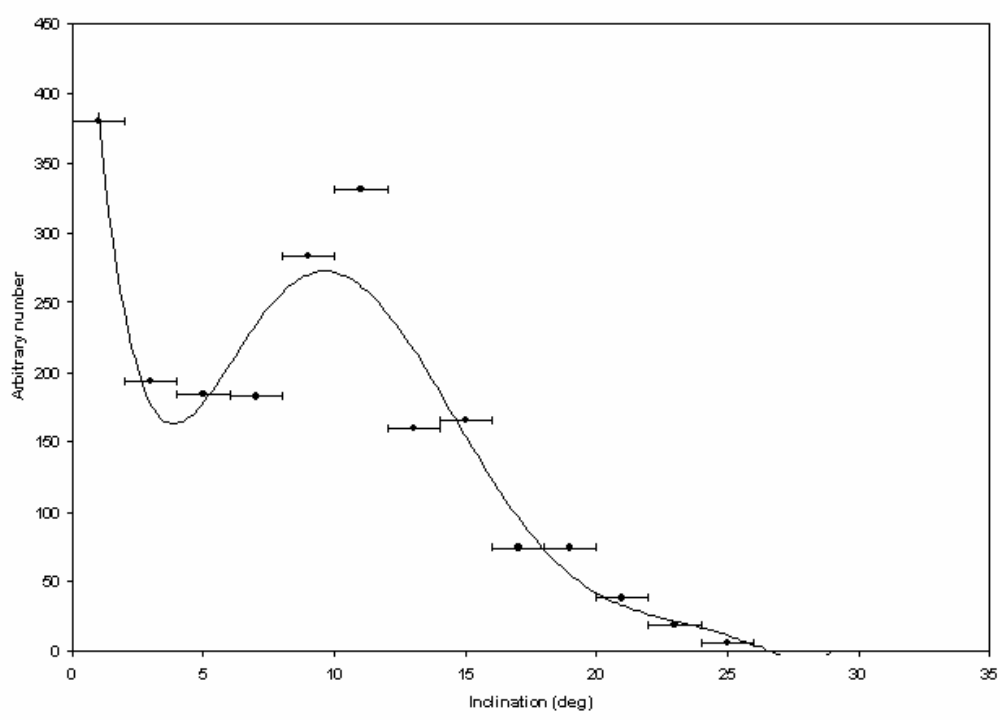

Figure 9.3 Distribution of orbital inclinations of 25μ asteroidal particles

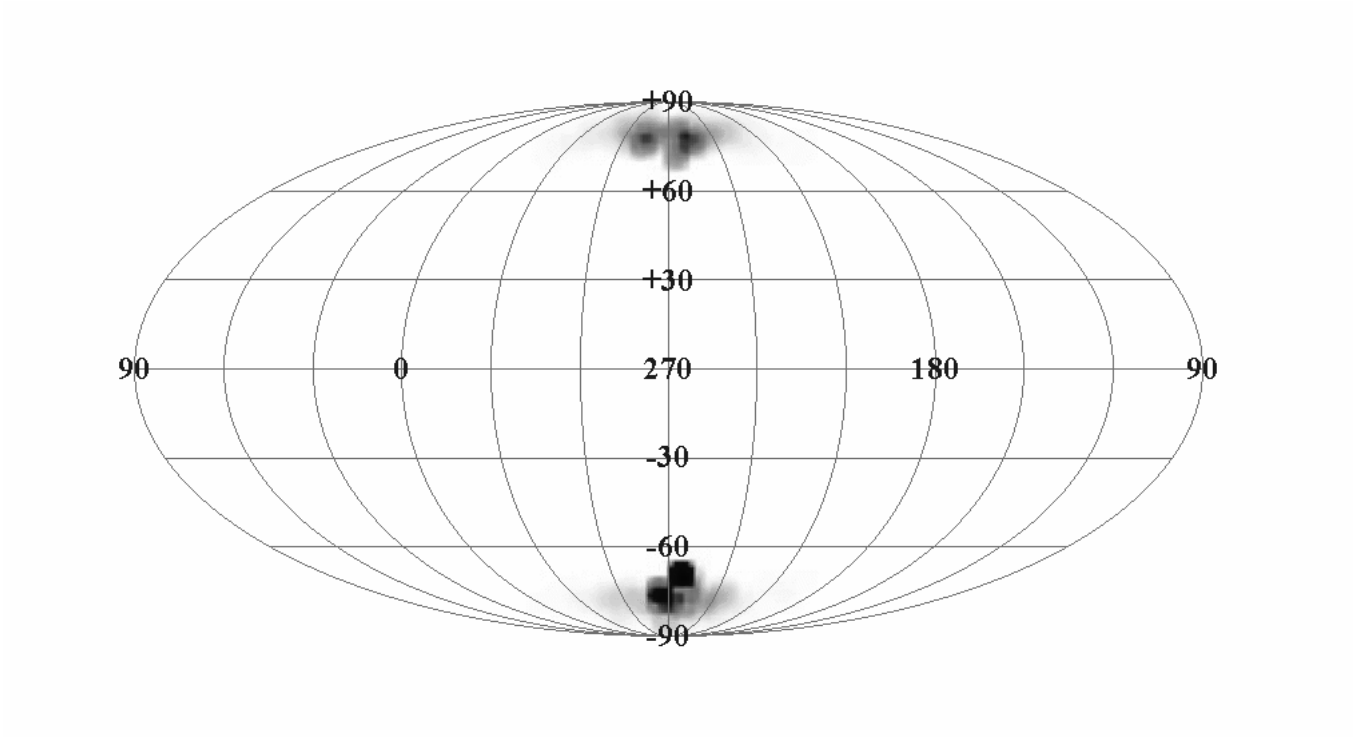

Figure 9.4 Predicted radiant distribution of asteroidal meteors as would be observed by an Earth-based meteor radar after the effects of the Earth's gravity and atmospheric deceleration have been removed.

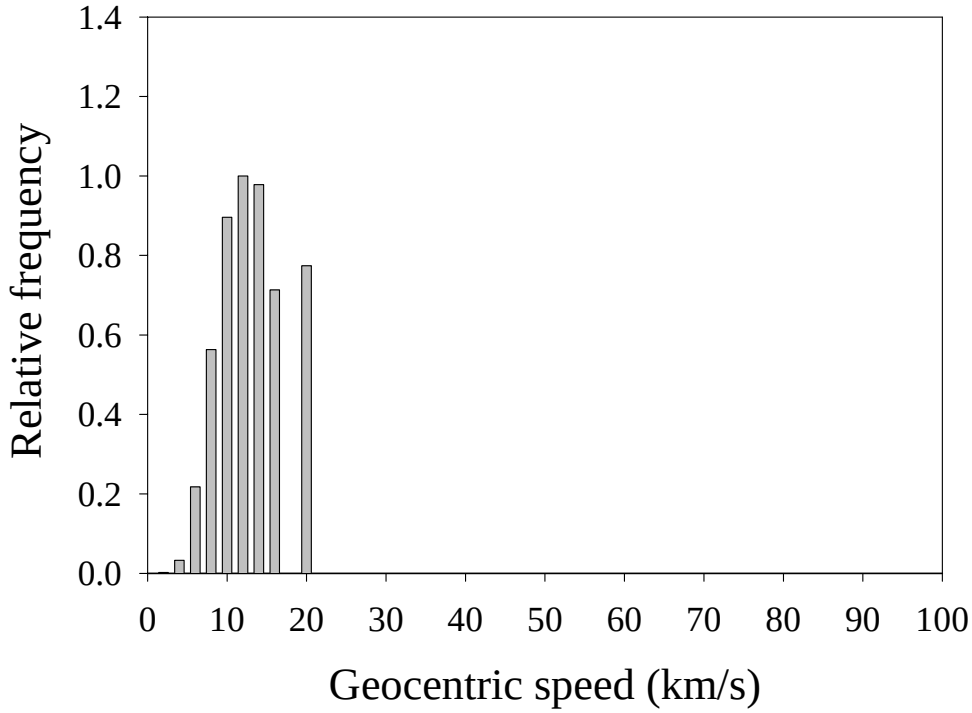

Figure 9.5 Predicted speed distribution of asteroidal meteoroids as would be observed by an Earth-based meteor radar after the effects of the Earth's gravity and atmospheric deceleration have been removed. The mean speed is 13.0 km/s.

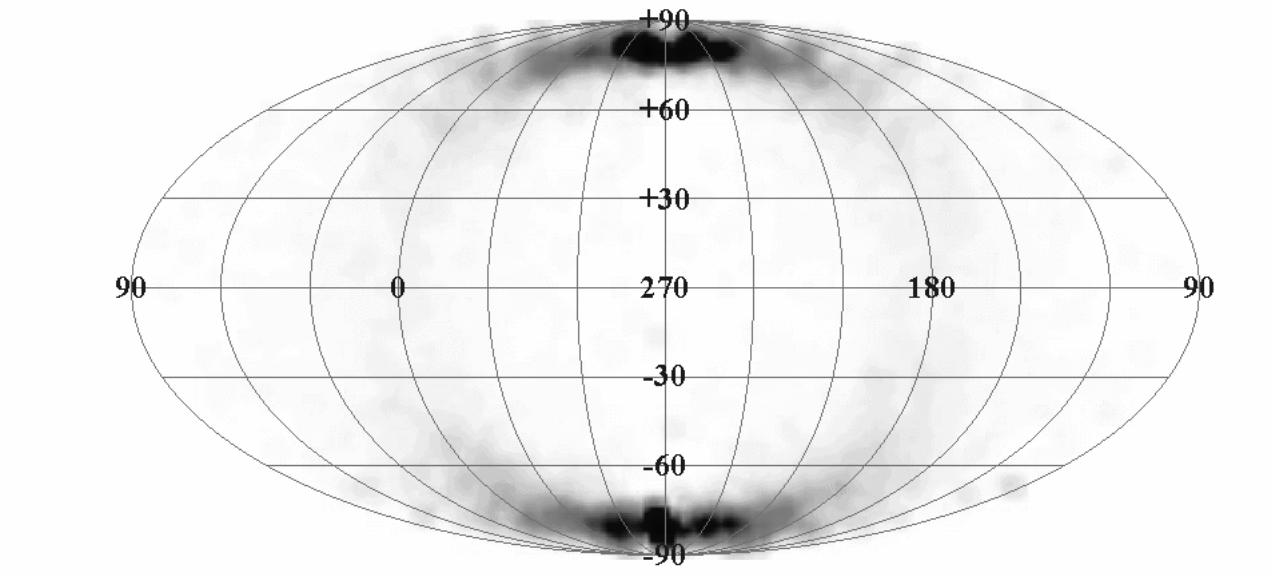

Figure 9.6 Predicted radiant distribution of asteroidal meteors as would be observed by an Earth-based mass-limited meteoroid detector after the effects of the Earth's gravity and atmospheric deceleration have been removed.

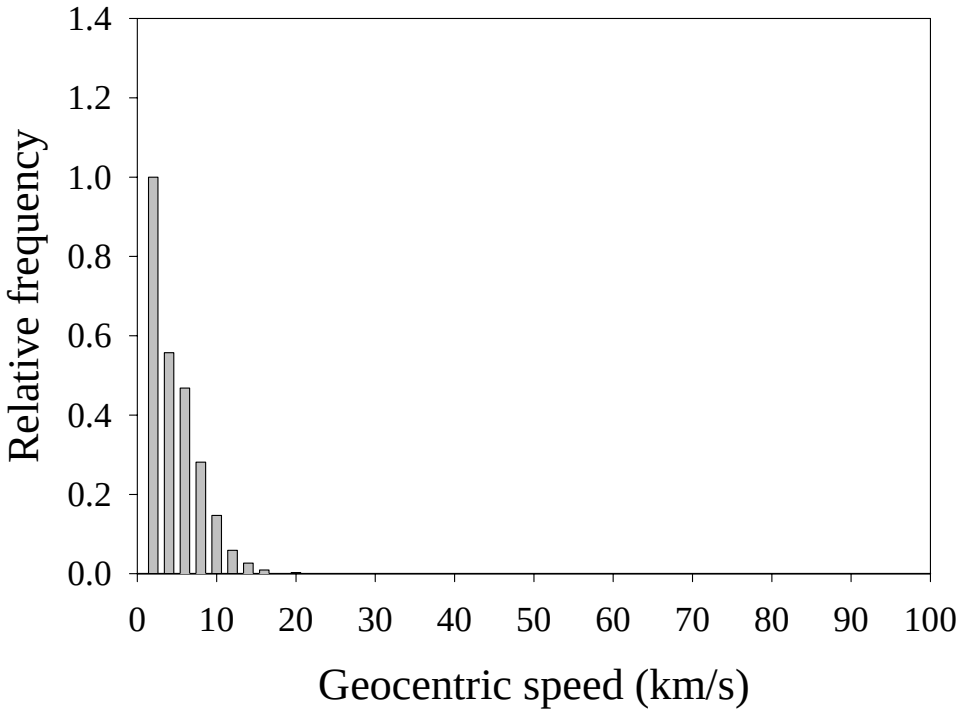

Figure 9.7 Predicted speed distribution of asteroidal meteoroids as would be observed by an Earth-based mass-limited meteoroid detector after the effects of the Earth's gravity and atmospheric deceleration have been removed. The mean speed is 4.7 km/s.

10. Gravitational focusing and shielding.

If the meteoroids approaching the space vehicle pass close to a planet, their trajectories may be altered significantly by the gravitational field of the planet so that both focussing and defocusing are possible depending on the geometry. It is also possible that the trajectory of the meteoroid may intersect the planet in which case it impacts with the planet and thus shields the vehicle. In this section we show how we have included both the effects of gravitational focussing and shielding in our model.

The first step in this treatment is to avoid complications arising from the different masses and sizes of the planets that are likely to be considered. We have adopted a unit of speed equal to that of a body in a circular orbit just above the surface of the planet. Our unit of distance is the radius of the planet.

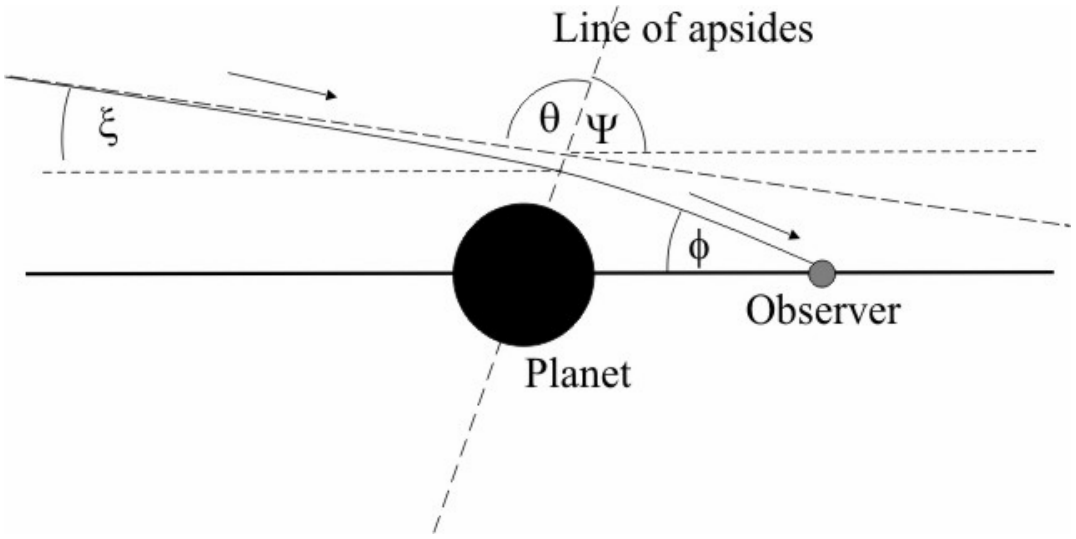

Figure 10.1 Focusing/shielding geometry

In this system of units, the trajectory is characterized by the parameter $F = v^2 r$ where v is the speed far from the planet and r is the distance of the observer from the planet. Using the principles of conservation of mechanical energy and angular momentum about the planet and much tedious algebra we obtain the following expressions for the various angles:

$$\cos(\theta) = -1/\sqrt{1 + F(F+2)\sin(\phi)^2} \tag{10.1}$$

$$\cos(\psi) = \frac{(F+2)\sin(\phi)^2 - 1}{\sqrt{1 + F(F+2)\sin(\phi)^2}} \tag{10.2}$$

Whereupon we find

$$\xi = 180 - \vartheta - \psi \tag{10.3}$$

This expression is inconvenient to use since in practice we will know the incident direction of the meteoroid (defined by ξ) and we wish to know its final direction (defined by ϕ). There are many methods that we could use to determine ϕ given ξ but our model involves large numbers of "particles" and we must take care that whatever technique we use does not slow the calculations down appreciably.

We chose to use a simple numerical approximation for $\phi(\xi,F)$ which depends on transforming ϕ and ξ by the variables ϕ_1 and ξ_1 given by

$$\phi_1 = \sqrt{(1-\cos(\phi)/2} \tag{10.4a}$$

and

$$\xi_1 = \sqrt{(1-\cos(\xi)/2} \tag{10.4b}$$

We find that the approximate numerical formula

$$\phi_1 \cong 0.6837\ (1-\xi_1)/\sqrt{F}\ (1+0.6\ \xi_1\sqrt{F}) \tag{10.5}$$

works well for F > 5 which covers the region of interest – for example 30 km/s at 2 Earth radii corresponds to a value of 28.7 for *F*. It will fail for low speeds close to the Earth but this is just the region when shielding will be more important than focussing. More work and time should yield even better approximate formulae. We are now in a position to determine the distribution of directions as seen by the observer given the initial distribution of directions.

If the trajectory of the meteoroid passes closer to the center of the planet than its radius, the observer will be shielded. This closest distance of approach, *q*, is given by

$$q = r\left(\sqrt{1+F(F+2)\sin(\phi)^2}-1\right)/F \tag{10.6}$$

If $q < 1.0$, we make the shielding weight, w_s, similar to the particle concentration weight defined by equation 5.6, of that "particle" to be zero.

The deflection process also changes the fluxes by virtue of its non-linearity. The geometry is shown in figure 10.2. The gravitational field of the planet causes the initially parallel bundle of trajectories begin to diverge so that the associated flux at the observer also changes as a result of the changing cross-sectional area of the bundle. These changes in the relative flux are conveniently dealt with by including them in the weighting coefficient and we therefore define a focussing weight, w_f, equal to the ratio of the cross-

sectional areas of the trajectory bundle at the observer to what it was before it was significantly deflected.

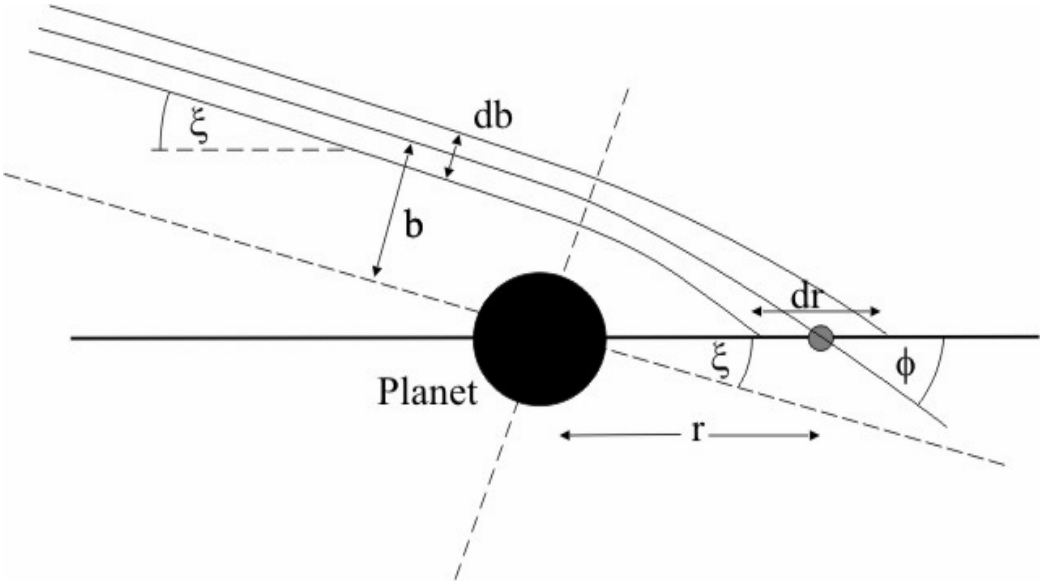

Figure 10.2 Focusing geometry: The gravitational field of the planet causes the initially parallel bundle of trajectories start to diverge.

The focussing weight is given by

$$w_f = \frac{b}{r \sin(\xi) \sin(\phi)} \frac{db}{dr} \tag{10.7}$$

where *b* is the impact parameter given by

$$b = r \sin(\phi) \sqrt{\frac{F+2}{F}} \tag{10.8}$$

Since the quantity $\sqrt{(F+2)/F}$ is only very weakly dependent on r, we can regard it as a constant so that

$$w_f \cong \sin(\phi) \left(F+2\right) / \sin(\xi)\, F \tag{10.9}$$

The composite weight used in the calculations is just the product of w_c, w_s *and* w_f.

Figures 10.3a – 10.3d show the effect of the focussing and shielding on the predicted radiant distribution for radio meteors at a distance of 20,000 km from the center of the Earth as it eclipses the helion source.

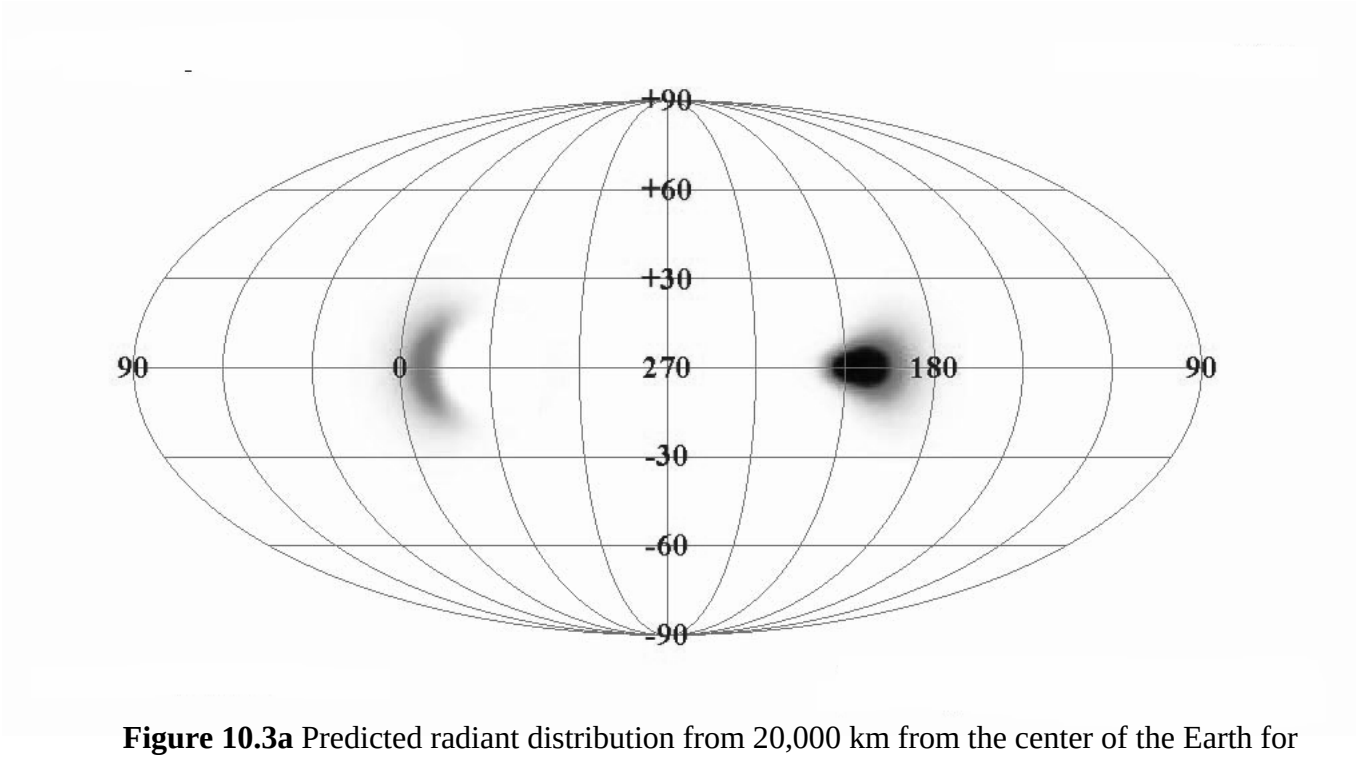

Figure 10.3a Predicted radiant distribution from 20,000 km from the center of the Earth for radio meteors as Earth eclipses the helion source. Earth at longitude 330^{o}**.**

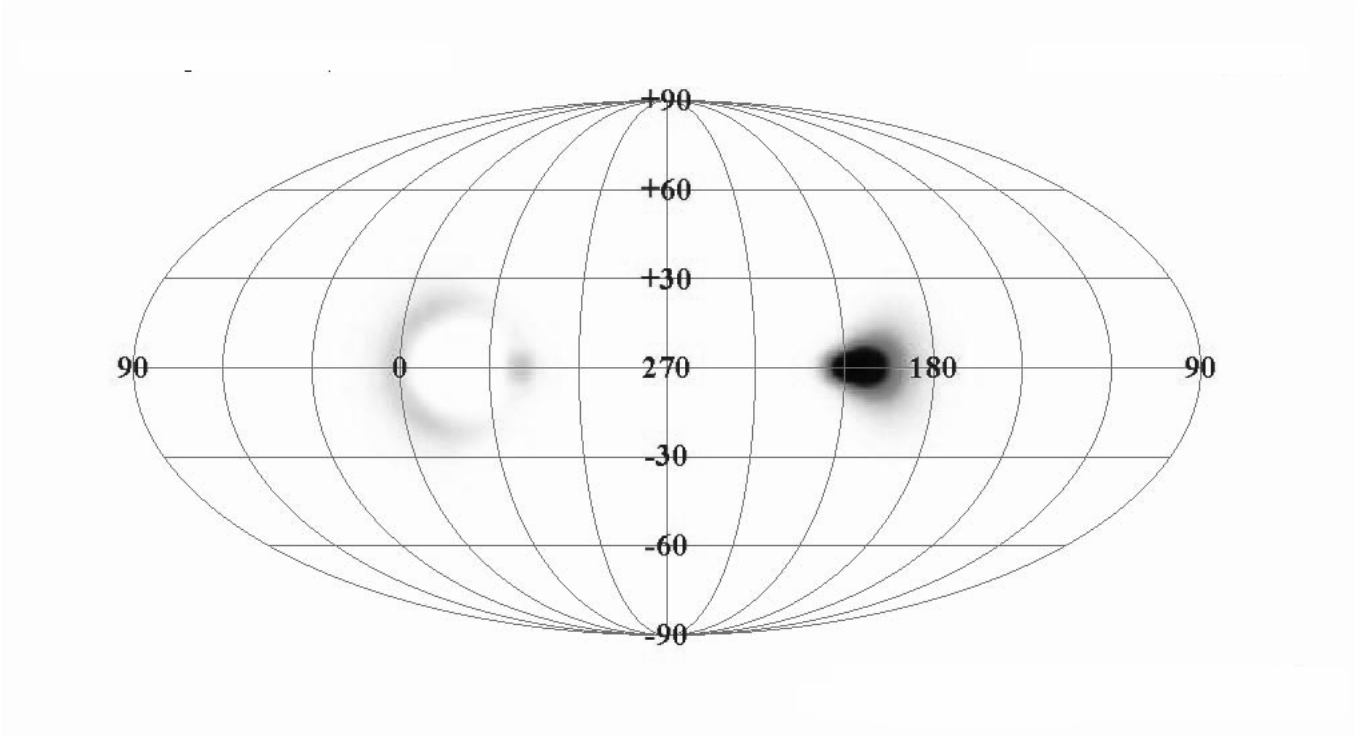

Figure 10.3b Predicted radiant distribution from 20,000 km from the center of the Earth for radio meteors as Earth eclipses the helion source. Earth at longitude 340^{o}.

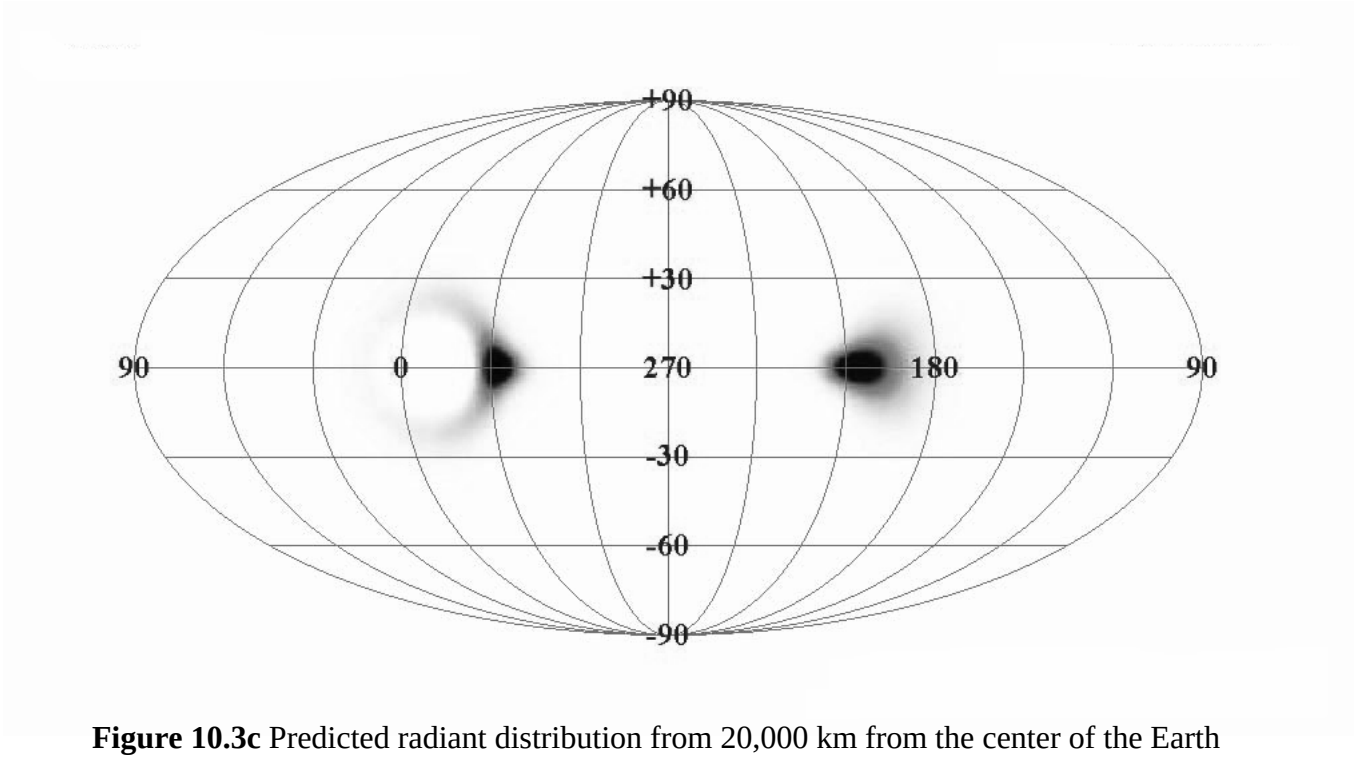

Figure 10.3c Predicted radiant distribution from 20,000 km from the center of the Earth for radio meteors as Earth eclipses the helion source. Earth at longitude 350^{o}.

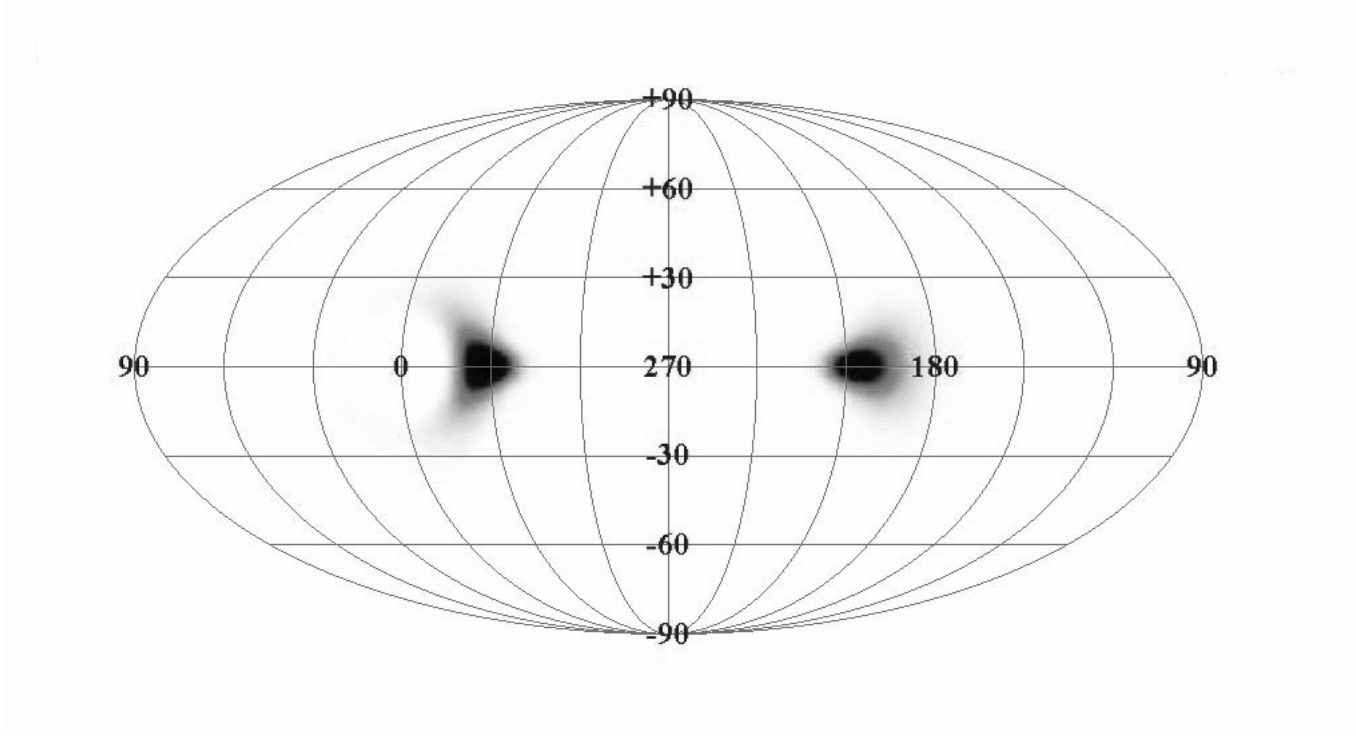

Figure 10.3d Predicted radiant distribution from 20,000 km from the center of the Earth for radio meteors as Earth eclipses the helion source. Earth at longitude 360^{o}.

It can be seen that depending on the location of the observer, he can experience a lower meteoroid flux because of shielding or an enhanced flux due to graviational focussing. As would be expected the shielding effect is most evident close to the planet on the opposite side to the source but the region of focussing extends to a distance of up to 10^6 km. The most affected region is along the axis joining the source and the planet up to a few hundred thousand kilometers. The focussing can enhance the flux of particles from the Helion source by as much as 70% as shown in figure 10.4 below.

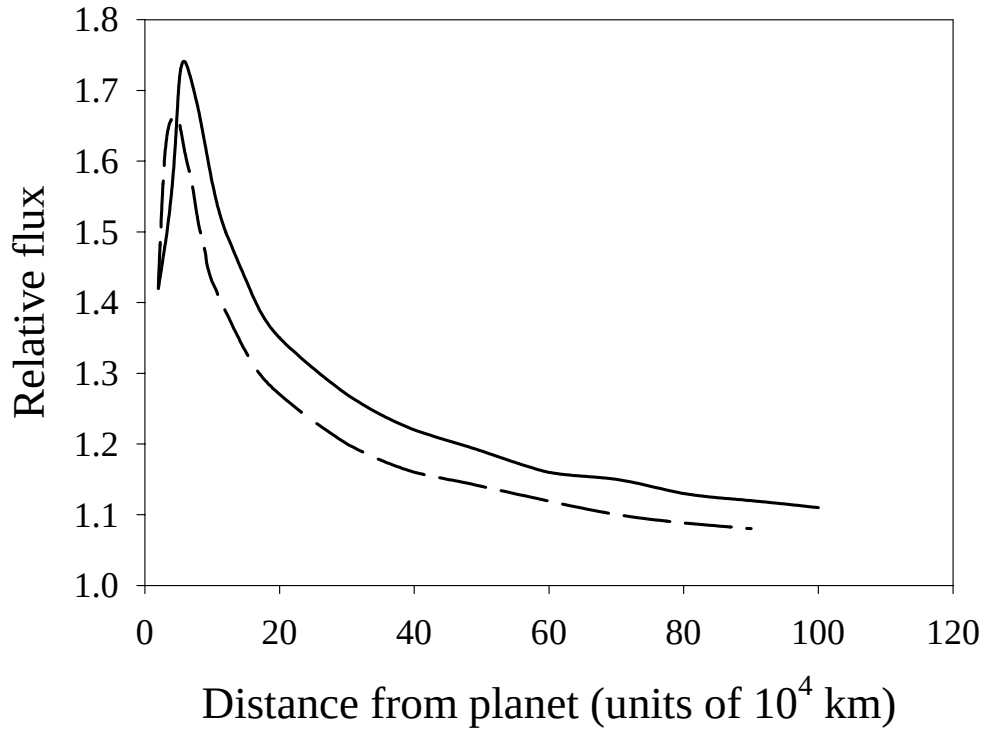

Figure 10.4 Enhancement of meteoroid flux due to gravitational focussing and shielding from the helion source versus distance from the Earth. The observer is moving with the same velocity as the Earth and is located on the axis joining the helion source and the Earth. The solid line is for ionization weighting while the dashed line is for mass weighting.

There is also enhancement of the flux transverse to the source-Earth line and this is shown in figure 10.5 which shows the the major part of the enhancement is limited to a range of longitudes of about 20^o. The slight asymmetry in the flux enhancement plot is the result of the asymmetry in the helion source.

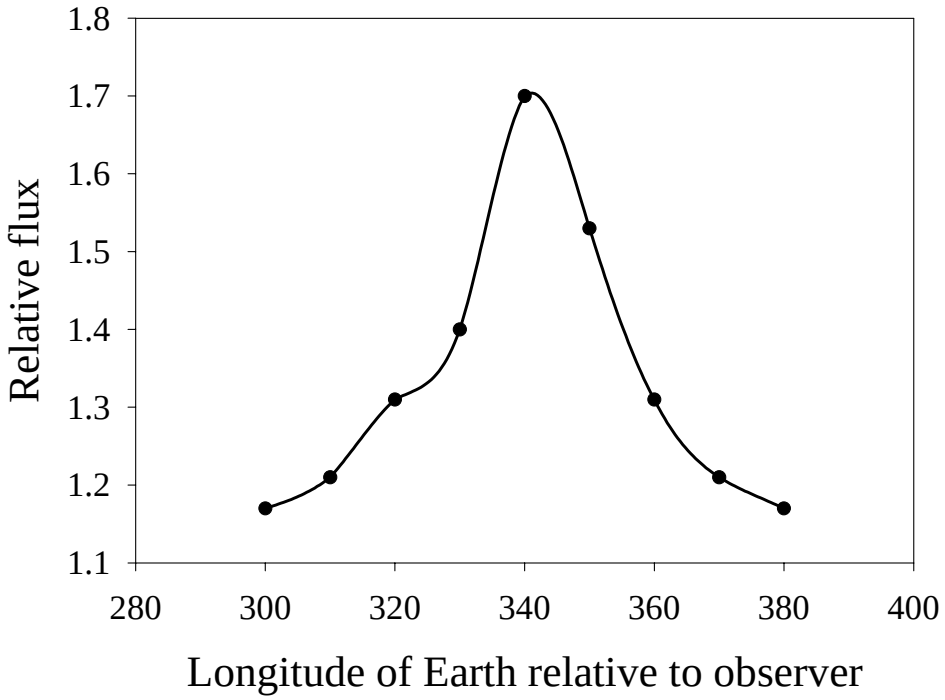

Figure 10.5 Enhancement of radio-meteor flux transverse to the source-Earth line. The observer is located 50,000 km from the center of the Earth and moving with the same velocity as the Earth. He is located and diametrically opposite to the helion source.

11. The software

The model is written as a collection of modules written in C which are integrated into a GUI written in Tcl/Tk. Tcl/Tk is a scripting language that allows applications to be developed rapidly without any deep knowledge of the Windows API. Indeed, Tcl/Tk is a cross-platform scripting language so that porting the software over to another platforms is a relatively straightforward task provided that the use of system-specific features have been avoided as is the case with SPORMOD. A good text is "Teach yourself Tcl/Tk in 24 hours" by Sastry and Sastry (SAMS) ISBN 0-672-31749-4. A great reference is the Tcl/Tk Programmer's Reference by Nelson (Osborne) ISBN 0-07-212004-5. The program also uses the Tcl/Tk extensions BLT and *img* and installation packages for MS Windows for these are on the CD. BLT is used for the bar chart plots while *img* is used for converting between image file formats. The program is written so that if the installation program provided is used, everything necessary for the program to run is installed automatically.

The Tcl/Tk script file is used to “glue” several applications together into a harmonious suite of programs so that the user is protected from the inner workings and is free to obtain the results he requires in a convenient fashion. Probably the most important task of

the script file is to provide the user with an intuitive mechanism for entering the relevant parameters such as direction, speed and heliocentric distance of the observing platform. He can also specify the weighting to be used – either mass or ionization and he can also set the sensitivity of his detectors as well as whether he wants to include the effects of gravitational shielding and focussing. All this sort of information is written to the *spormod.cfg* file that is used extensively by other modules of the program.

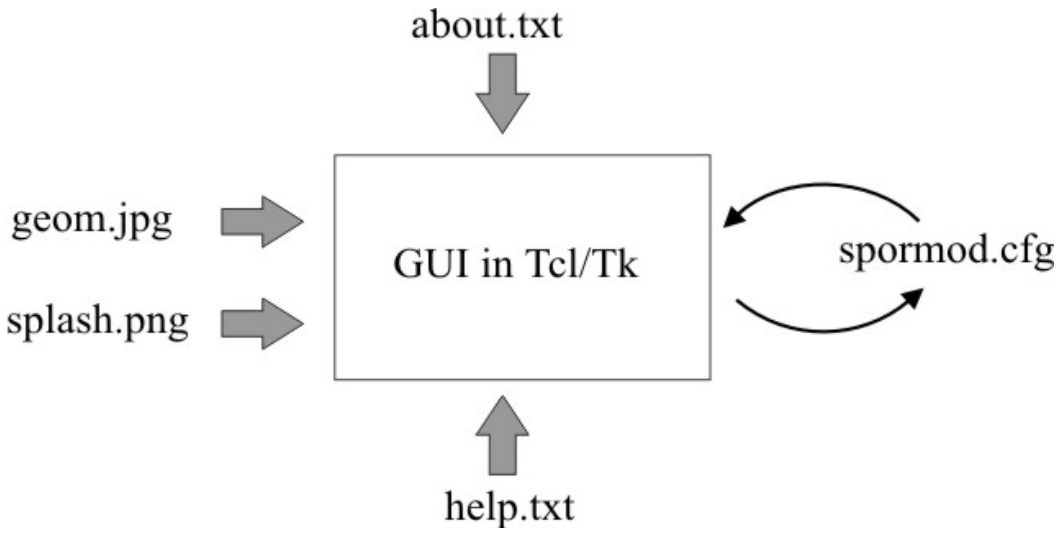

Figure 11.1 Files involved with the main Graphical User Interface (GUI)

The installation is very straightforward as the CD is setup for auto-installation. If for some reason the host computer has the auto-installation feature disabled the setup can be initiated by double clicking on the SetupSporMod3 icon in the CD directory.

The application is can be invoked in several ways – either from the command line from the c:\SporMod3\bin\ directory with the command wish82 spormod.tcl. A much more convenient method is to use the SporMod3 shortcut on the Desktop that makes use of a small C program -spormod.exe - to invoke the Tcl/Tk interpreter and the associated scripts.

The model consists of two main sections: orbit generation and orbit analysis. Five hundred thousand orbits are generated in each set.

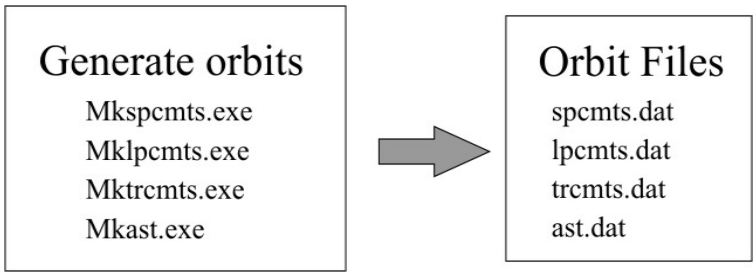

Figure 11.2 Files involved in the generation of orbits.

The analysis engine is *mkmapsetc.exe* which takes as its input the orbit files, a configuration file and the *xpm.hdr* files and produces both *xpm* image files as well as *?vdist.dat* files which contain the speed distribution for "meteoroids" from each source. The configuration file *spormod.cfg* contains a list of variables which depend on the user's choice of settings and which are also used to restore the settings to the previous state when the program is invoked. The *xpm.hdr* file is used in the construction of the *xpm* image files of the radiant distributions.

The final step in the analysis is to calculate the fluxes and this is accomplished by the *srcrat.exe* program which takes as its input the speed distribution files and the *spormod.cfg* files *srcrat.exe* produces an output file *fluxes.dat* which contains the fluxes of the various sources at either a magnitude of +6.5 if the program has been configured for ionization weighting or to 1 g in the case of mass weighting. The conversion has been calibrated using the radio meteor data from the CMOR radar operated by the UWO meteor group. The calculation of the fluxes for arbitrary magnitudes and masses is carried out in the Tcl/Tk program.

All the data and configuration files are ASCII files that have been annotated as much as possible.

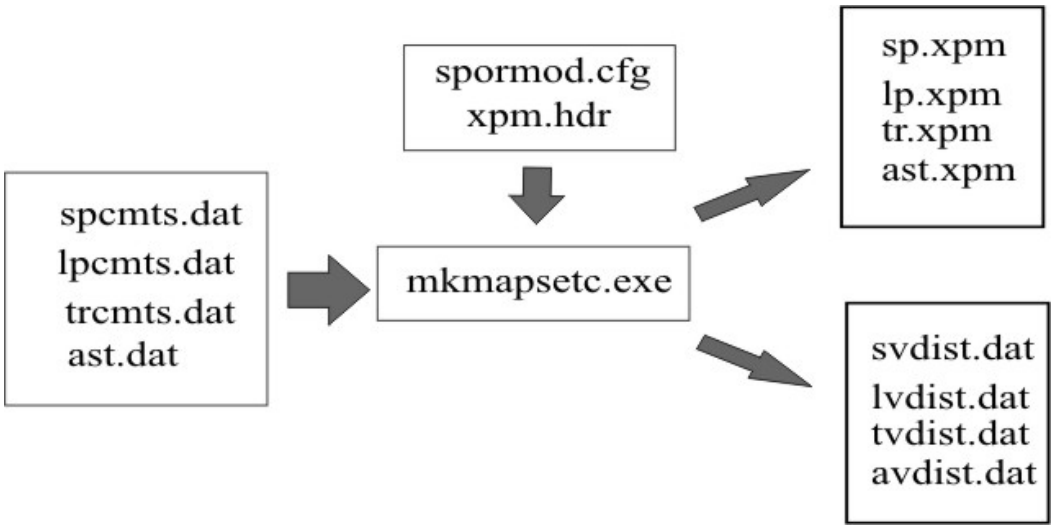

Figure 11.3 Files used in the first stage of the analysis. The *.xpm files are image files with the radiant distributions and the *vdist.dat files contain the speed distributions of the "meteoroids" from the various sources

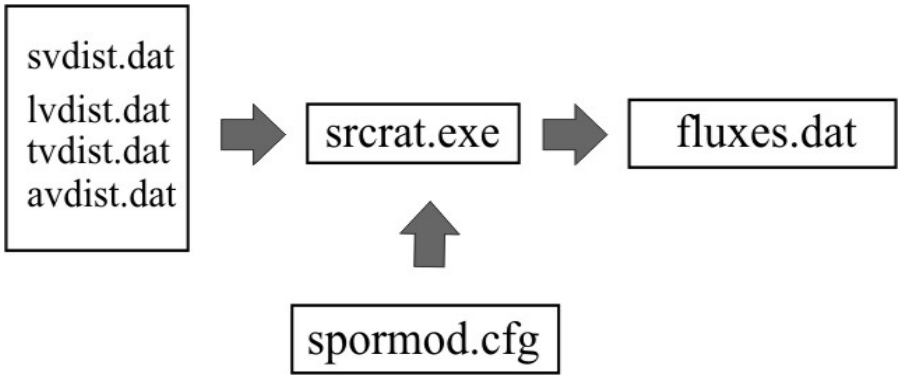

Figure 11.4 Files used for calculating the fluxes at either +6.5 M (ionization weighting) or 1 g (mass weighting).

12. Conclusions

SPORMOD is a model of the complex of meteoric particles in the inner Solar System based upon our knowledge of comets, the sublimation of the cometary ices, the evolution of the orbits of the particles released from comets under the action of the Poynting-Robertson effect and some heuristic ideas of how collisions limit the lifetimes of these cometary particles. Because our knowledge is incomplete, we have described our model

in terms of a few parameters that we have been able to determine by finding a best fit with the very recent observations of the CMOR meteor radar operated by the UWO meteor group. The model is by no means the final word if for no other reason that the CMOR is still a system in its infancy and the analysis procedures are being constantly refined.

Even in its present state, CMOR is able to produce 6000 orbits per day - a factor of 6 better than any other meteor radar has performed. The most similar radar is AMOR, operated by Dr. W.J. Baggaley in Christchurch, NZ. However because of its special antenna system, AMOR sees only a very small fraction of shower meteors and has to depend on other means to estimate the accuracy of the speed measurements. Shower meteors on the other hand are very prominent on the CMOR radar and we therefore have a very reliable “ground truth” for our measurements of meteoroid speeds. At the moment we confident that we can reduce the errors in our measured speed to significantly below 10%.

Several of the parameters of the model depend strongly on the observed mean speed of meteors. The inclusion of correction for the attenuation due to the initial radius effect increases the mean speed of the meteoroids significantly. So even though the corrections are not large in themselves, they have a relative large effect on the model parameters. On the other hand we have not had the time to investigate whether the uncertainty in the parameters have a correspondingly large effect on the final equilibrium orbital distributions.

One area that deserves some attention is that of the radiant imaging of the CMOR observations since that would afford some confirmation of our determinations of the model parameters. We are very confident that single station determinations of the radiant distribution are superior to those from the three-station system. Jones (1993) devised a very powerful method to extract radiant distributions from single-station observations. This, combined with the very accurate interferometer system (Jones, Webster and Hocking, 1999), yields radiant distributions with higher resolution than those obtained from individual radiants with the three-station system. This apparently anomalous result comes about because the three-station system uses time delays as well as the interferometer to determine the meteor trajectories so introducing another source of measurement error. The author plans to rewrite this single-station imaging software to incorporate several new ideas that will allow the parameters of the sources to be determined much more accurately.

Another area that would make the model much easier to use would be to modify it so that a file with the itinerary of a space vehicle could be read into the program that would allow the directionality and strength of the fluxes to be calculated on a day-by-day basis throughout the mission.

An important contribution of this work has been the development of a method to deal quantitatively with the effects of gravitational shielding and focussing. For sporadic meteors observed from the Earth the rates can be enhanced by as much as 70%. For

meteor streams, which are highly collimated, the enhancement can be much greater. This is an area that deserves more study and could provide the solution to long-standing problems such as the 45 minute period in which Mariner IV experienced unusually high impact rates.

One of the main assumptions we have made that we know to be incorrect is that the sporadic meteoroid complex is azimuthally symmetric about the ecliptic pole. It has been known for over five decades that the sporadic meteor activity varies in a systematic fashion through the year. The fact that this is the same in both northern and southern hemispheres shows that this is a real effect and that there is a considerable azimuthal variation in the particle concentration. The variation is not small being more than a factor of 2. It needs to be included since it can be more important than gravitational shielding and focussing but how we can include it is not obvious at the present.

As it stands the model applies only to an observer moving in the ecliptic. There is obvious benefit for space vehicles to move out of the ecliptic in order to avoid the relatively dense cloud of meteoric particles. The extension of the model to cover this case, although straightforward in principle, nevertheless involves some awkward geometric considerations.

Finally some thought should be given to the extension of the model beyond the orbit of Jupiter. The main difficulty with this is the scarcity of observations in this region. But since we see that the meteoroid environment at Earth can be satisfactorily described in terms of cometary sources, we might expect that extrapolation to this region may not be as reckless as it might appear at first sight. We know that in this region long-period and Halley family comets are likely to be the main contributors to the dust environment.

In conclusion, we are very happy with the progress of the development of the model and are frankly amazed that so much progress has been possible with such limited data.

13. References

1. Baggaley, W.J., Bennett, R.G.T., Steel, D.I., and Taylor, A.D., 1994, Q.J.R.astr. Soc. 35, 293 – 320.

2. Brown, P. 1994. M.Sc Thesis. University of Western Ontario.

3. Campbell-Brown, M.P. and Jones, J. 2003, MNRAS, {*in press*}

4. Delsemme, A.H., 1976, Lecture Notes Phys. 48, 314.

5. Devine, N. 1993. Geophys. Res. 98 (E9), 17029 - 17048.

6. Everhart, E. 1967b. Astr. J., 72, 1002.

7. Garrett, H.B., Drouilhet, S.J., Oliver, J.P., Evans, R.W., 1999, J. Spacer. Rockets 36, 124 - 132.
8. Greenhow, J.S. and Hall, J.E. 1960, MNRAS 121, 183 – 196.

9. Grün, E., Zook, H.A., Fectig, H. and Giese, R.H. 1985, Icarus, 62 244-272

10. Hughes, D.W. 1987, MNRAS 226, 309 - 316.

11. Jehn, R. 2000, Planet. Space. Sci., 48, 1429 - 1435.

12. Jones, J. 1993. Presented at Asteroids Comets and Meteoroids in Versailles. Abstract published in proceeding.

13. Jones, J. 1995, MNRAS 275, 773 - 780.

14. Jones, J. and Brown, P. 1993, MNRAS 265, 530.

15. Jones, J. Ellis, K. Webster, A.R. and Brown, P. and Campbell, M. 2002, {in preparation}

16. Jones, J. Webster, A.R. and Hocking, W.K. 1998, Radio Sci., 33, 55 – 65.

17. Jones, W. 1997. MNRAS 288, 995.

18. Kessler, D.J. 1981, Icarus, 48, 39.

19. Leinert, C., Rösser, S. and Buitrago, J. 1983, Astron. Astrophys. 118, 345-357.

20. Lindblad, B.A. 1987, Publ. Astron. Inst. Azech., 67, 201.

21. Marsden, B. A 1989, Catalog of Cometary Orbits, Cambridge, Mass. Smithsonian Astrophysical Observatory

22. Öpik, E.J. 1951, Proc. Roy. Irish Acad. 54, 165

23. Sekanina, Z. 1976, Icarus, 27, 265.

24. Steel, D.I. and Elford, W.G. 1986, MNRAS 265, 530.

25. Stohl, J. 1968, in Physics and Dynamics of Meteors p 298. Eds L Kresak and P.M. Millman. Reidel, Dordrecht, Holland.

26. Taylor, A.D. 1995, Icarus, 116, 154-158.

27. Verniani, F. Smithon. Contrib. Astrophys. 8, 141.

28. Whipple, F.W. 1967, in The Zodiacal Light and Interplanetary Medium, ed J.L.Weinberg, NASA SP-150, Washington, p.409

29. Wyatt, S.P. and Whipple, F.L. Astrophys. J. 1950, 111, 134.